Russian Chemical Reviews **72** (9) 735 – 757 (2003) © 2003 Russian Academy of Sciences and Turpion Ltd

DOI 10.1070/RC2003v072n09ABEH000775

Molecular models of solvation in polar liquids

G N Chuev, M V Basilevsky

Contents

I.	Introduction	735
II.	General scheme for the calculation of solvation	736
III.	Continuum models	737
IV.	Method of integral equations	740
V.	Electrostatic interactions in the Monte Carlo and molecular dynamics methods	741
VI.	Hydrophobic effects	742
VII.	Solvation of ions	744
VIII.	Polar molecules	747
IX.	Solvated quantum particles	748
X.	Tautomeric and conformational equilibria	749
XI.	Electronic spectra and solvatochromic shifts	750
XII.	Electron transfer	751
XIII.	Conclusion	753

Abstract. The state-of-the-art theory of solvation in polar liquids is considered. The main molecular models and protocols for the calculation of solvation are presented. The protocols based on advanced electrostatic models of solvation, the use of correlation functions found by solving the integral equations of statistical physics and the numerical modelling of solvation processes using Monte Carlo and molecular dynamics methods are described. Attention is focused on the application of the above models to the thermodynamics of the solvation of ions and hydrophobic and polar molecules. Peculiarities of the modelling of processes related to solvation such as electron transfer, conformational and tautomeric equilibria, and solvatochromic shifts in the electronic spectra of the solvated molecules are discussed. The bibliography includes 325 references.

I. Introduction

The character of interaction of a solute with the solvent during solvation depends on the physicochemical properties of solutions and liquid-phase associates. Vast experimental material on the solvation of various molecular objects has been accumulated to date; numerous data on the effect of the solvent on the structural and spectral parameters of the solute molecules, the kinetics and mechanisms of chemical and biochemical reactions are documented. Suffice it to say that in only one monograph [1] devoted to the solvation effects in organic chemistry, does the number of references exceed 2500. According to the Institute of Scientific Information (Philadelphia, USA), more than 10 000 papers on the topic 'solvation' are published annually in scientific journals.

Solvation of molecules is accompanied by various physicochemical processes.[2,3] A solvation shell is formed around each molecule. The physical properties of the solvent can substantially change — dissociation or association of molecules can take place, and the conformations and the electronic structures of both solvated species and solvent species can be affected. This gives rise to diverse specific solvation effects. On the basis of the enormous body of experimental data, a large number of solvation models have been constructed, which are used for interpretation of different solvation effects.

Starting with the Born model,[4] theoretical studies of solvation for one-atomic ions have long been based on the continuum model of the medium. In recent years, considerable advances have been made along this line related to the improvement of the existing and development of new protocols for the calculation of solvation effects. The general trend is to take into account the molecular structure of the solvent. Description of the solvent at the molecular level can be implemented either within the bounds of continuum approximations, which are vivid and simple as regards the calculations, or on the basis of a consistent statistical theory (the method of integral equations). A special place belongs to the numerical simulation of the solvation effects by molecular dynamics (MD) or Monte Carlo (MC) techniques, which are used more and more often as the computing machinery develops.

The improvement of the simple continuum solvation schemes proposed previously gives rise to an hierarchy of phenomenological approximations, intermediate between these simplest schemes and true molecular theories of solvation. Particular applications of the theory of solvation make use (not always critically) of the whole range of the available methods of this theory. The purpose of this review is to analyse and describe systematically the results obtained using the molecular models of solvation proposed recently.

The review can be divided conventionally into three parts that include Sections II – V, VI – IX and X – XII, respectively. The first part outlines the general scheme for the calculation of solvation

G N Chuev Institute of Theoretical and Experimental Biophysics, Russian Academy of Sciences, 142292 Pushchino, Moscow Region, Russian Federation. Fax (7-096) 739 05 53. Tel. (7-096) 773 91 09.
E-mail: genchuev@rambler.ru
M V Basilevsky State Scientific Centre of the Russian Federation 'L Ya Karpov Institute of Physical Chemistry', ul. Vorontsovo Pole 10, 105064 Moscow, Russian Federation. Fax (7-095) 975 24 50.
Tel. (7-095) 917 39 03. E-mail: basil@cc.nifhi.ac.ru

Received 4 October 2002
Uspekhi Khimii **72** (9) 827 – 851 (2003); translated by Z P Bobkova

and describes the calculation of solvation processes on the basis of upgraded continuum models and integral equations. Since voluminous literature on the MD and MC numerical simulation techniques is available (see, for example, Refs 5–14), we have not discussed here their principles and engineering implementations, but, as an exception, have touched upon the problems of taking into account the electrostatic interactions within the framework of these methods and have briefly considered the calculation of the change in the thermodynamic functions upon solvation — this aspect is especially important for chemical and biological applications. The second part dealing with hydrophobic effects provides a brief description of thermodynamic integration, which is an efficient up-to-date algorithm of such calculations, and considers typical objects to which various methods of solvation theory are applied, depending on the conditions. These objects can be represented by hydrophobic molecules, ions, polar molecules and quantum particles (solvated electrons, bipolarons and positronium). The third part is devoted to the study of processes related to solvation (electron transfer, conformational and tautomeric equilibria and solvatochromic shifts in the electronic spectra). The prospects for using the molecular models of solvation in polar liquids are considered in the Conclusion.

In order to maintain a reasonable relationship between the coverage of information and the logics of narration, we restricted the scope of this review to analysis of the key methods of the solvation theory and did not dwell on detailed discussion of the results obtained.

II. General scheme for the calculation of solvation

The choice of the intermolecular interaction potentials plays a crucial role in the theory of solvation. In most solvation theories, particles of the solute [15] and the solvent (both atoms and molecules) are considered within the framework of classical mechanics. The set of methods and calculation algorithms involved are often referred to as 'molecular mechanics' (MM).[16,17] In this case, it is suggested most often that these potentials can be represented as sums of effective atom–atom pair potentials

$$U(\boldsymbol{R}^{\{N\}}) = \sum_{I \neq J}^{N} u(|\boldsymbol{R}_I - \boldsymbol{R}_J|).$$

Here $U(\boldsymbol{R}^{\{N\}})$ is the potential energy of the solute–solvent system, N is the total number of atoms in the system, $\boldsymbol{R}_I$ and $\boldsymbol{R}_J$ are the radius-vectors of atoms I and J, respectively. The summation covered every possible pair of atoms where both atoms belong to either the solute or a solvent molecule, or one atom belongs to the solute and the other one, to the solvent molecule. The indices I and J imply simultaneously the type and the number of an atom. An advantage of this approach is the possibility of finally reducing the problem to the study of only radial atom–atom potential functions. However, even in this approximation, parametrisation of the interatomic force fields is very complicated. This requires specification of the functional form of each potential containing adjusting parameters, which are selected by comparing the results of trial calculations with the experimental data on the structure and thermodynamic properties of one-atomic and molecular liquids. A number of parametrisation protocols for the intra- and intermolecular force fields (AMBER,[18] CHARMM,[19] OPLS,[20] GROMOS,[21] GROMACS,[22] *etc.*) have been developed. These techniques make use of the partial charges of atoms q_i for parametrisation of the Coulomb interaction and the Lennard-Jones model for parametrisation of the non-Coulomb contribution to atom–atom potentials.

The main phase in the calculation of classical molecular models is determination of the equilibrium ensemble of atomic configurations

$$\overline{\boldsymbol{R}}^{\{N\}} = \overline{\boldsymbol{R}}_1 \overline{\boldsymbol{R}}_2 \ldots \overline{\boldsymbol{R}}_N$$

in a chosen volume of the medium either by solving dynamic equations (MD method) or using the MC method. In both cases, the final outcome is the calculated atom–atom (AA) correlation function (CF) $g_{AB}(|\boldsymbol{R}_1 - \boldsymbol{R}_2|)$, which is related to the conditional probability that one atom A of some molecule will be found at point $\boldsymbol{R}_1$ provided that atom B of another molecule occurs at point $\boldsymbol{R}_2$.[23]

The presence of chemical bonds gives rise to correlations that are specified by intramolecular correlation functions (IMCF). For rigid molecules, IMCF depends only on the molecular geometry, while for non-rigid molecules, averaging of these functions over all molecular conformations should be carried out. The atom–atom correlation functions (AACF) and the IMCF provide full information on the local microscopic structure of the solution and the solvated complex. All thermodynamic values (Gibbs energy of solvation ΔG, chemical potential μ and so on) can also be calculated from the correlation functions and the intra- and intermolecular interaction potentials.[23]

More detailed investigations of real solvation systems require a quantum-mechanical (QM) calculation of electron density distribution $\rho_e(\boldsymbol{r})$ and many-electron wave function $\Psi(\boldsymbol{r}^{\{n\}})$ (n is the number of electrons). However, the quantum-chemical calculations from 'primary principles' are very laborious and can now be carried out only for systems consisting of several tens of atoms. For systems comprising hundreds of atoms, semiempirical methods are employed. Therefore, hybrid (QM/MM) methods, *i.e.*, calculation protocols that use simultaneously the equations of quantum and molecular (classical) mechanics, are now actively used to study solvation. All molecules of the solution are divided into two subsystems, namely, the solute (for which the quantum calculations are carried out) and the solvent, which is described on the basis of classical molecular models. Correspondingly, quantum (Q), classical (M) and mixed (QM) contributions to the intermolecular potentials are distinguished. The full Hamiltonian H of the system includes each of these contributions.

$$H = H_Q + H_{QM} + H_M, \tag{1}$$

$$H_Q = \sum_i \frac{\boldsymbol{P}_i^2}{2m_i} + \sum_{ij} \frac{Z_i Z_j}{|\boldsymbol{R}_i - \boldsymbol{R}_j|} + \langle \Psi | H_e | \Psi \rangle,$$

$$H_{QM} = \sum_{iI} \left[\frac{Z_i q_I}{|\boldsymbol{R}_i - \boldsymbol{R}_I|} - \left\langle \Psi \left| \frac{q_I}{|\boldsymbol{r}_i - \boldsymbol{R}_I|} \right| \Psi \right\rangle + V(|\boldsymbol{R}_i - \boldsymbol{R}_I|) \right],$$

$$H_M = \sum_I \frac{\boldsymbol{P}_I^2}{2m_I} + \sum_{IJ} u(|\boldsymbol{R}_I - \boldsymbol{R}_J|).$$

Here, the subscripts i, j, I, J refer to atoms of the quantum and classical subsystems, respectively; $\boldsymbol{P}_i$, $\boldsymbol{P}_I$ and $\boldsymbol{R}_i$, $\boldsymbol{R}_I$ are the impulses and coordinates (radius-vectors) of atoms; Z_i, m_i are the charge and the mass of the solute nuclei, H_e is the electron Hamiltonian (we do not write it out in an explicit form) and the brackets $\langle \Psi | \ldots | \Psi \rangle$ mean averaging over the electronic configuration of the solute with coordinates of the electrons r_i. The operator H_{QM} contains both the electrostatic (the first two terms) and non-electrostatic (V) contributions.

The use of Hamiltonian (1) implies the calculation of the many-electron wave function Ψ and the equilibrium configuration $\overline{\boldsymbol{R}}^{\{N\}}$ of the solvent molecules. In terms of the method of correlation functions, the problem of solvation can be reduced to the investigation of the effective Hamiltonian H_{ef}, which governs the behaviour of the quantum subsystem in the external field $V_{ef}(\boldsymbol{R})$ created by solvent molecules at point $\boldsymbol{R}_i$,

$$H_{ef} = H_Q + V_{ef} = \sum_i \frac{\boldsymbol{P}_i^2}{2m_i} + \sum_{ij} \frac{Z_i Z_j}{|\boldsymbol{R}_i - \boldsymbol{R}_j|} + \tag{2}$$

$$+ \langle \Psi | H_e | \Psi \rangle + \sum_{AB} \int g_{AB}(\boldsymbol{r}) u_{AB}(|\boldsymbol{r} - \boldsymbol{R}|) \mathrm{d}\boldsymbol{r},$$

where $g_{AB}(\boldsymbol{r})$ is the AACF between atoms of the solvated complex and the solvent and $u_{AB}(\boldsymbol{r})$ are the corresponding atom–atom potentials. The free Gibbs energy of solvation of the system (per solute species) is given by the equation

$$\Delta G = \langle \Psi | H_{ef} | \Psi \rangle - \langle \Psi_0 | H_Q | \Psi_0 \rangle + \mu, \tag{3}$$

where $\Psi_0(\boldsymbol{r}^{\{n\}})$ and $\Psi(\boldsymbol{r}^{\{n\}})$ are many-electron wave functions of the solute in vacuum and in the solvent, respectively, μ is the chemical potential of the solvent, which can be expressed in terms of the CF. Since the AACF is determined by the equilibrium configuration of the solvent molecules, which also depends on the electron density distribution $\rho_e(\boldsymbol{r})$, self-consistent calculation of Ψ and $g_{AB}(\boldsymbol{r})$ is required. The calculation procedure is as follows. Some initial approximation is taken for the wave function Ψ and for the spatial configuration of the solute. The next stage is to calculate the charge distribution on the solute atoms, to find the equilibrium configuration $\overline{\boldsymbol{R}}^{\{N\}}$ and $g_{AB}(\boldsymbol{r})$, to calculate the external field and, finally, to correct Ψ by calculating the electron density distribution in this external field. This procedure should be repeated until full self-consistence is attained. Various modifications of this procedure are related to the choice of methods for calculating $g_{AB}(\boldsymbol{r})$ (MD, MC or integral equations) and Ψ. The allowance made for electron polarisation of the solvent molecule changes appreciably the whole calculation scheme.

In the general case, the calculation of the equilibrium configuration of the solute + solvent system, like the calculation of the AACF, is labour-consuming; therefore, additional simplifications are used in continuum models. The approximations based on the linear response theory [24] allow one to reduce the problem to the calculation of the wave function Ψ in the reactive self-consistent field (SCF) V_{ef}, which depends on the dielectric constant of the liquid and charge distribution in the solute. Thus, using continuum models (CM), one can calculate the energy of solvation and the electron density distribution on the solvated molecule without calculating the correlation functions. Actually, this requires only an additional self-consistent calculation of V_{ef}, which can be naturally included into standard quantum-chemical procedures.[25]

III. Continuum models

The linear response approximation in the theory of solvation appears to be justified for considering the electrostatic interactions in the system consisting of a solute and the solvent. It is widely used for systems where such interactions predominate, *i.e.*, for charged and highly polar solutes in polar solvents. This approximation forms the basis for the continuum theory. It is formulated as a relationship between the charge distribution on the solute $\rho_Z(\boldsymbol{r})$, which depends on the charge of the atomic nuclei and the electron density distribution $\rho_e(\boldsymbol{r})$, *i.e.*,

$$\rho_Z(\boldsymbol{r}) = \sum_i Z_i \delta(\boldsymbol{r} - \boldsymbol{R}_i) - \rho_e(\boldsymbol{r}),$$

and the field of the medium 'response' $V(\boldsymbol{r})$, *i.e.*, electrostatic field

$$V(\boldsymbol{r}) = \widehat{K}\rho_Z = \int \rho_Z(\boldsymbol{r}') K(\boldsymbol{r}, \boldsymbol{r}') \mathrm{d}\boldsymbol{r}'. \tag{4}$$

Here $\widehat{K}$ is the linear integral operator with a symmetric nucleus $K(\boldsymbol{r}, \boldsymbol{r}')$ (the Coulomb Green function, which has the following form for the case of electrostatic potential in vacuum: $|\boldsymbol{r} - \boldsymbol{r}'|^{-1}$). Within the linear theory, the Helmholtz free energy of solvation is equal to

$$\Delta F = \frac{1}{2}\int \rho_Z(\boldsymbol{r}) V(\boldsymbol{r}) \mathrm{d}\boldsymbol{r} = \frac{1}{2}\int \rho_Z(\boldsymbol{r}') K(\boldsymbol{r}, \boldsymbol{r}') \rho_Z(\boldsymbol{r}) \mathrm{d}\boldsymbol{r}' \mathrm{d}\boldsymbol{r}. \tag{5}$$

In the simplest case of a homogeneous medium, the charge distribution $\rho_Z(\boldsymbol{r})$ is related to the induction field $\boldsymbol{D}(\boldsymbol{r})$ by the Poisson equation

$$\nabla \boldsymbol{D} = 4\pi\rho_Z(\boldsymbol{r}), \tag{6}$$

and the polarisation $\boldsymbol{P}(\boldsymbol{r})$ of the medium is equal to

$$\boldsymbol{P}(\boldsymbol{r}) = \frac{1}{4}\pi\left(1 - \frac{1}{\varepsilon_0}\right)\boldsymbol{D}(\boldsymbol{r}), \tag{7}$$

$$\boldsymbol{D} = \varepsilon_0 \boldsymbol{E},$$

where ε_0 is the static dielectric constant of the solvent, $\boldsymbol{E}$ is the electric field. A variable polarisation arises in a homogeneous medium as the response field. This simple model has found wide application in early versions of the electron transfer theory.

To describe the solvation effects at an up-to-date level, one should take into account the discrete (atomic) structure of the solvated molecule. There appears a boundary separating the region occupied by the solute (the 'cavity' in which the dielectric constant ε is taken to be unity) from the surrounding area filled with a continuous medium with $\varepsilon = \varepsilon_0$. With such boundary conditions, it is inconvenient to use the variables $\boldsymbol{P}(\boldsymbol{r})$ and $\boldsymbol{D}(\boldsymbol{r})$, and transition to the general relations (4) and (5) is expedient. In this case, the response nucleus $K(\boldsymbol{r}, \boldsymbol{r}')$ is defined as the function ε_0. The numerical implementation of this procedure is equivalent to the solution of the Poisson equation with the appropriate boundary conditions, which can be different depending on the particular method used to specify the boundary of the cavity accommodating the solute. Some of these methods are mentioned below.

A more general formulation of electrostatic equations is proposed in non-local electrostatics.[26,27] For a homogeneous medium, simple relations (6) and (7) are replaced by the relation

$$\boldsymbol{P}(\boldsymbol{r}) = \int \boldsymbol{E}(\boldsymbol{r}') \chi(\boldsymbol{r} - \boldsymbol{r}') \mathrm{d}\boldsymbol{r}'. \tag{8}$$

Here $\chi(\boldsymbol{r} - \boldsymbol{r}')$ is the non-local generalised dielectric susceptibility. In the standard phenomenological approach,[26–29] it is expressed in terms of the dielectric function $\chi(\boldsymbol{k})$ [Fourier transform of the function $\chi(\boldsymbol{r})$], which is in turn related to the dielectric susceptibility $\varepsilon(\boldsymbol{k})$ in the following way:

$$\chi(\boldsymbol{k}) = \frac{1}{4\pi}\left[1 - \frac{1}{\varepsilon(\boldsymbol{k})}\right]. \tag{9}$$

This approach allows one to take into account the structure of the medium in the continuum theory. As an example, we consider the model function $\chi(\boldsymbol{k})$ for the isotropic case where it depends only on the length of the vector $\boldsymbol{k}$. In the simplest variant, this model has the form [24–30]

$$\chi(\boldsymbol{k}) = \chi_0 + \frac{\chi_1}{1 + k^2\varsigma^2}. \tag{10}$$

Here χ_0 and χ_1 are constants, the former determining the local, while the latter, the non-local components of the susceptibility; $k = |\boldsymbol{k}|$; the model parameter ς is the correlation length. After the backward transformation, the Fourier function (10) gives rise to a 'susceptibility kernel,' which depends only on the distance between the points $\boldsymbol{r}$ and $\boldsymbol{r}'$

$$\chi(|\boldsymbol{r} - \boldsymbol{r}'|) = \chi_0 \delta(\boldsymbol{r} - \boldsymbol{r}') + \frac{\chi_1}{4\pi\varsigma^2|\boldsymbol{r} - \boldsymbol{r}'|} \exp\left(-\varsigma^{-1}|\boldsymbol{r} - \boldsymbol{r}'|\right), \tag{11}$$

where δ is the Dirac delta function.

In conformity with relation (8), the response $\boldsymbol{P}(\boldsymbol{r})$ decays exponentially with an increase in the distance $|\boldsymbol{r} - \boldsymbol{r}'|$, and the dielectric shielding of the solute charge is efficient only at distances not exceeding ς. In the description of the orientational polarisation of the medium, the ς value is of the order of the characteristic size of the solvent particles.

The applicability of local models is restricted by the limited case $\varsigma \lesssim \varsigma_0$, where ς_0 is the characteristic size of the solvated molecule. By introducing multimodal model functions as the sums of Lorentzian functions (10) with different parameters $\varsigma_1, \varsigma_2, \ldots$, equation (10) can be generalised to describe the structure of the solvent around the solute in more detail.[24–28]The non-local models for an inhomogeneous medium are complex and have

been developed only for spherically symmetric systems,[30–33] although the equations describing them are also known for the general case.[31–33] In these models, linear relation (4), and, finally, (leaving aside the technical complexity), the response nucleus $K(\boldsymbol{r},\boldsymbol{r}')$ can be expressed in terms of the function $\chi(\boldsymbol{k})$ or $\varepsilon(\boldsymbol{k})$.

This type of approach can be extended to time-dependent effects by introducing the functions $\chi(\boldsymbol{k},\omega)$ or $\varepsilon(\boldsymbol{k},\omega)$ that depend on the frequency ω. In the absence of spatial dispersion, they are reduced to the functions $\chi(\omega)$ and $\varepsilon(\omega)$, which are complex values.[34] For example,

$$\varepsilon(\omega) = \varepsilon_1(\omega) + \varepsilon_2(\omega),$$

where the terms ε_1 (real) and ε_2 (imaginary) are even and odd functions of ω, respectively. The transition to time functions is performed by the Fourier inversion.

Relation (4) also holds for molecular theories if the applicability conditions of the linear response are met. Then the nucleus $K(\boldsymbol{r},\boldsymbol{r}')$ can be calculated within the framework of one or another microscopic model. In the classical limit, the Kirkwood formula holds,[34,35] which expresses the nucleus of the integral operator $\widehat{K}$ in terms of the correlation function $\langle \Delta V(\boldsymbol{r})\Delta V(\boldsymbol{r}')\rangle_{\rho_Z T}$ of fluctuations of the microscopic electric field

$$K(\boldsymbol{r},\boldsymbol{r}') = -\beta\langle \Delta V(\boldsymbol{r})\Delta V(\boldsymbol{r}')\rangle_{\rho_Z T}, \tag{12}$$

where $\beta = (k_B T)^{-1}$, k_B is the Boltzmann constant; averaging involves an ensemble with fixed charge density distribution ρ_Z and temperature T. Relation (12) allows one to perform MC or MD simulation of the nucleus $K(\boldsymbol{r},\boldsymbol{r}')$ on the basis of calculations of the correlation function $\langle \Delta V(\boldsymbol{r})\Delta V(\boldsymbol{r}')\rangle$. Finally, it becomes possible to transfer the approaches developed in the continuum theory to molecular models.

Of all the existing computation schemes, the continuum theory most simply, although roughly, takes into account the solvation effects. Owing to the simplicity of the numerical procedure, continuum models have been widely distributed and underlie a large number of applied computer programs. Here, we only briefly touch on different versions of continuum models, because voluminous literature devoted to this topic is available.[36–43]

Continuum models can be classified in terms of the procedure of calculation of the reactive self-consistent field V_{ef} acting upon the solute [see Eqn (2)]; in terms of the method of inclusion of the short-range contribution V_s; or in terms of the numerical procedure used to calculate the wave functions Ψ. In addition, in the calculations that are meant to provide the semiquantitative agreement with the experiment, the cavity accommodating the solute should have a complex shape 'adjusted' to the real solute structure; hence, a procedure for finding this cavity is also required.

Quantum-chemical calculations for the solvated complex use most often *ab initio* computations based on the Hartree–Fock (HF) approximation supplemented by some scheme for taking into account the electron correlations.[44–49] In many publications, the Ψ functions are calculated in terms of the density functional theory (DFT).[50–53]

Comparison of the data obtained by different methods shows a substantial scatter of the results (Table 1), which is, however, due not only to the calculation scheme chosen but also to the use of different parameters for the interatomic interaction potentials. The results of both HF and DFT calculations are in almost equally satisfactory agreement with the experimental data.

The ways of taking into account the short-range contribution V_s depend on the way of parametrisation of the van der Waals interactions. Most often, the Solvent Accessible Surface (SAS) approximation is used according to which the contribution of short-range forces to ΔG (ΔG_s) is proportional to the solute surface area accessible to the solvent molecules. If the SAS has a complex shape, it is considered as consisting of separate S_i fragments, which correspond to the solute atoms, and ΔG_s is calculated as the sum over the fragments [60]

Table 1. Experimental and calculated [by DFT, MM, HF, SMx (Solvation Model) and CM methods] values of free energy ΔG (kcal mol^{-1}) for the hydration of amines and amides.

Solute	Experiment (see [54])	Calculation by the method					
		DFT (see [53])	MM (see [55])	HF (see [56])	SMx (see [57])	MM (see [58])	CM (see [59])
NH_3	−4.3	−4.8	−4.0	−5.1	−4.3	−4.2	−6.3
CH_3NH_2	−4.6	−3.0	−3.7	3.5	–	−3.5	−4.5
$(CH_3)_2NH$	−4.3	–	−1.2	–	−4.3	−1.9	−2.7
$(CH_3)_3N$	−3.2	–	−0.6	–	−2.6	0.4	−1.2
Acetamide	−9.7	−9.0	−11.9	−9.2	–	–	−9.8
NMA [a]	−10.1	–	−9.3	–	–	–	−7.8
NNDMA [b]	−8.5	–	−7.3	–	–	–	−6.3

[a] NMA is *N*-methylacetamide; [b] NNDMA is *N*,*N*-dimethylacetamide.

$$\Delta G_s = \sum_i A_i S_i\,, \tag{13}$$

where A_i is a coefficient expressed in the surface tension units. According to the Generalised Born Surface Area (GBSA) model,[61,62] it is assumed that the A_i value is determined only by the type of atom. In more advanced SMx models,[63,64] it depends additionally on the type and length of the bonds and (implicitly) on the charge of the *i*th atom. Attempts have been made to parametrise the separate contributions related to the repulsion of atoms and to their attraction due to dispersion interactions. The complexity of such calculations is obvious, due to the fact that these contributions have opposite signs and partially neutralise each other. In some cases, these contributions are expressed *via* one- and two-electron integrals for the corresponding atomic orbitals and are included in the calculation scheme as a component of the self-consistent field acting on the solute.[65] The repulsion contribution contains a temperature-dependent 'non-potential' component, namely, the cavitation energy (see Section VI). Other methods for the parametrisation of ΔG_s also exist. Comparative analysis of the existing methods showed [66] that, with appropriate thoroughness, they all provide similar estimates of ΔG_s .

A number of modifications of continuum models exist, depending on the procedure of calculation of the self-consistent field, which is dictated by the method used to solve the Poisson equation for the electrostatic potential V_{ef} created by the charge distribution $\rho_Z(\boldsymbol{R})$

$$\nabla\varepsilon(\boldsymbol{R})\nabla V_{ef}(\boldsymbol{R}) = -4\pi\rho_Z(\boldsymbol{R}). \tag{14}$$

This equation corresponds to the most general case where the dielectric constant of the (inhomogeneous) medium $\varepsilon(\mathrm{R})$ depends (unlike ε_0) on the spatial coordinates R. Equation (14) can be numerically solved by using various finite-difference schemes or the finite-element method. This way of solving the equation is, however, labour-consuming, because elucidating the details of field distribution $V_{ef}(\boldsymbol{R})$ requires the use of a three-dimensional network with a large number of points.[67] In some cases, poor convergence is observed during the solution. Despite these drawbacks, this approach has quite a lot of supporters, especially among researchers engaged in molecular biology,[59] which is due to the availability of the relevant program packages for the solution of the Poisson–Boltzmann [68] and Poisson [69] equations.

Most often, the cavities of the solute excluded volume are considered, the dielectric constant being a stepwise function

$$\varepsilon(R) = 1$$

inside the cavity and

$$\varepsilon(R) = \varepsilon_0$$

outside the cavity. Then for a spherical cavity with the radius a, the solution of Eqn (14) can be written as a multipole expansion into spherical harmonics $Y_l^m(\psi,\theta)$ [38, 70]

$$V_{\text{ef}}(R>a)=\sum_{l=0}^{\infty}\frac{2l+1}{l+(l+1)\varepsilon}\,\frac{1}{R^{l+1}}\sum_{m=-l}^{l}B_{lm}Y_l^m(\psi,\theta),$$

$$V_{\text{ef}}(R\leqslant a)=V_0(\boldsymbol{R})+V_\sigma(\boldsymbol{R})=\sum_{l=0}^{\infty}\frac{1}{R^{l+1}}\sum_{m=-l}^{l}B_{lm}Y_l^m(\psi,\theta)+$$

$$+\sum_{l=0}^{\infty}\frac{(l+1)(\varepsilon-1)}{l+(l+1)\varepsilon}\,\frac{1}{a^{2l+1}}\sum_{m=-l}^{l}B_{lm}Y_l^m(\psi,\theta), \qquad (15)$$

where $R=|\boldsymbol{R}|$, B_{lm} are the expansion coefficients. In relation (15), the contributions $V_0(\boldsymbol{R})$ and $V_\sigma(\boldsymbol{R})$ represent the potential created by the charge distribution on the solute in vacuum and the response field created by the induced charge of the surface of the sphere, respectively. In the case of a solute with an arbitrary shape, one can use a multicentred multipole expansion.[38] In this case, the whole surface of the solute is first split into spherical fragments for which expansion (15) is performed, while the self-consistent field $V_{\text{ef}}(\boldsymbol{R})$ is calculated as a superposition of the contributions of all centres. An essential drawback of this approach is poor convergence of series (15); as a consequence, it is difficult to control the number of terms of the series needed to ensure the specified precision. For small molecules, an accuracy of not less than 93% is attained at $l_{\max}=8$ (see Ref. 71), whereas for large molecules, $l_{\max}$ increases linearly with an increase in the distance from the expansion centres. The case where only the terms with $l_{\max}=0$ are considered corresponds to the Born approximation [4] and $l_{\max}=1$, to the Onsager approximation.[72] The two last-mentioned protocols are embodied in a large number of computer programs. The former underlies the GBSA model (generalised Born model taking into account the accessible surface),[60] which is actively used for 'classical' calculations of the solvation energy of biomacromolecules [73] or the energy of binding of a ligand to a protein.[74] Yet another example is represented by SMx models [62] where this approximation is used for the quantum-chemical calculation of solvation. Note that the results of calculations in terms of these models are highly sensitive to the choice of the a radius.

An alternative method for solving the Poisson equation is the popular Polarised Continuum Model (PCM).[75–78] According to this model, the solute is immersed in a cavity with a complex shape which is constructed as a combination of (overlapping) spheres drawn around each of the solute atoms. The radii of the spheres are expressed in terms of the van der Waals radii of atoms by introducing a scaling multiplier, which is a method parameter. Equation (14) with the function $\varepsilon(\boldsymbol{R})$, which acquires different constant values inside and outside the cavity, is reduced to the integral relation

$$V_\sigma(\boldsymbol{R})=V_{\text{ef}}(\boldsymbol{R})-V_0(\boldsymbol{R})=\int_S\frac{\sigma(\boldsymbol{R}')}{|\boldsymbol{R}-\boldsymbol{R}'|}\,\mathrm{d}\boldsymbol{R}'. \qquad (16)$$

Here, S is the surface area of the boundary of the cavity around the solute over which the corresponding surface integral is calculated.

It follows from electrostatics equations that the surface charge $\sigma(\boldsymbol{R}')$ on the boundary of the cavity is related to the field strength $E(\boldsymbol{R}')$ by the relation

$$\sigma(\boldsymbol{R}')=\frac{1-\varepsilon_0}{4\pi\varepsilon_0}\boldsymbol{n}(\boldsymbol{R}')E(\boldsymbol{R}')= \qquad (17)$$

$$=\frac{\varepsilon_0-1}{4\pi\varepsilon_0}\boldsymbol{n}(\boldsymbol{R}')\nabla\big[V_0(\boldsymbol{R}')-V_\sigma(\boldsymbol{R}')\big],$$

where $\boldsymbol{n}(\boldsymbol{R}')$ is the unit vector of the inward normal to the surface S. Equations (16) and (17) taken in combination provide the possibility of obtaining a closed-loop iterative scheme for the calculation of $\sigma(\boldsymbol{R}')$ and $V_\sigma(\boldsymbol{R}')$.

The key integral equation of the PCM determines the surface charge $\sigma(\boldsymbol{R})$ (see Ref. 79)

$$\sigma(\boldsymbol{R})=\frac{1-\varepsilon_0}{4\pi\varepsilon_0}\left[\int_V a(\boldsymbol{R},\boldsymbol{R}')\rho_z(\boldsymbol{R}')\mathrm{d}\boldsymbol{R}'+\right. \qquad (18)$$

$$\left.+\int_S a(\boldsymbol{R},\boldsymbol{R}')\sigma(\boldsymbol{R}')\mathrm{d}^2\boldsymbol{R}'+2\pi\sigma(\boldsymbol{R})\right],$$

$$a(\boldsymbol{R},\boldsymbol{R}')=\frac{\partial}{\partial\boldsymbol{n}(\boldsymbol{R})}\left(\frac{1}{|\boldsymbol{R}-\boldsymbol{R}'|}\right),$$

where a is the normal derivative of the Coulomb potential.

The right-hand part of Eqn (18) is the sum of volume and surface integrals.

Iterative algorithms are used most often to solve Eqns (16) and (17) for $V_\sigma(\boldsymbol{R})$ and $\sigma(\boldsymbol{R}')$ or the equivalent equation (18) for $\sigma(\boldsymbol{R})$. The function $\sigma(\boldsymbol{R})$ is approximated by the network of its values on small segments of the surface S. In some existing alternative (non-iterative) calculation schemes, the set of the $\sigma(\boldsymbol{R})$ values on the segments of the cavity surrounding the solute is considered as a vector and the Eqns (16), (17) and (18) that determine it are reduced to a high-dimension matrix equation (see the review [36] and the references cited therein).

The PCM model is represented by a large number of versions whose comparative analysis has been reported.[37] A recent version [80] makes it possible to carry out the calculation of solvation in liquid crystals and salt solutions. A simplified modification of the PCM is the Conductor-Like Screening Model (COSMO),[81] which assumes that highly polar liquids such as water ($\varepsilon_0=80$) can be regarded as conductors ($\varepsilon_0=\infty$). The corresponding equation for the charge surface density obtained in terms of this model is solved by the matrix method mentioned above. This scheme is considered to be attractive for calculating the solvation of large biomacromolecules.[82]

To conclude the Section, let us turn back to the problem of applicability of the linear response theory to the description of solvation. The linear approximation is basic for the use of continuum models; its adequacy was verified by comparing the results of calculations in terms of these models with the results of MD or MC calculations.[83–85] Comparison showed a substantial deviation of the response from linearity. The deviation is smaller for charged solvated molecules than for polar molecules; in addition, the non-linearity of the real response increases with a decrease in the solute charge. Before the publications,[83–85] it was believed that non-linear effects should arise in strong electric fields (dielectric saturation). Calculations [84, 85] revealed an absolutely different effect of purely molecular nature generated in weak fields. It was found that linearity of the dielectric response is violated due to solvent structurisation in the near environment of the solute caused by short-range van der Waals interactions. As the strength of the external electric field increases, a 'phase transition' takes place and the linearity is restored. However, studies were carried out only for aqueous solutions, and it is unknown whether this effect is significant for non-aqueous systems.

Apparently, continuum models cannot provide a calculation accuracy above 80% for either free or potential energy, or for the electrostatic potential, irrespective of the way of parametrisation of the non-electrostatic contribution or the shape of the solute cavity. One more shortcoming of the continuum models is that they do not allow one to estimate temperature dependences of the energy of solvation or to study the change in the local structure of the solution near the solute. Nevertheless, due to the relative simplicity of the calculation of ΔG and the possibility of estimating the changes in the electronic structure of the solute, the continuum models appear rather attractive for applications, especially in the field of biochemistry and molecular biology.

IV. Method of integral equations

The MC or MD calculation of the correlation functions is associated with a great amount of computation. By using the CF formalism, it is possible to reduce the problem to a simpler investigation of Ornstein–Zernike type equations.[23,86,87] These equations relate the atom–atom radial distribution function $g(r)$ to the 'direct' correlation function $c(r)$, which plays an important role in the statistical mechanics and determines the two-particle spatial correlations (medium density) caused by the interatomic potential $u(r)$ so that $c(r \to \infty) \to -\beta u(r)$. In the case of an infinitely dilute solution where a monoatomic solute in a monoatomic liquid is considered, the equation for the $h_{AB}(r) = g_{AB}(r) - 1$ (see †) is written in the form

$$\gamma_{AB}(R) = h_{AB}(R) - c_{AB}(R) = \rho \iint c_{AB}(r) h_{BB}(|\boldsymbol{r} - \boldsymbol{R}|) \mathrm{d}\boldsymbol{r}, \qquad (19)$$

where ρ is the average solution density, $h_{BB}(r)$ is the full correlation function of the pure solvent. The integral equation (19) connects two functions, h and c, and, hence, it can be supplemented by the 'closure' condition. This condition can be obtained as the dependence of the function c_{AB} on the 'bridge' functional B

$$c_{AB} = \exp[-\beta u_{AB} + \gamma_{AB} + B(\gamma_{AB})] - \gamma_{AB} - 1.$$

No exact expression for the bridge functional has yet been found; however, a large number of approximate expressions have been obtained for simple liquids by the diagram expansion method;[88,89] the applicability of such expressions is limited to the $u(r)$ type of interaction. For example, the hyperchain (HC) approximation (HCA) with $B[\gamma(r)] = 0$ is used for long-range interactions and $B[\gamma(r)] = \ln[1 + \gamma(r)] - \gamma(r)$ corresponds to the Percus–Yevick (PY) approximation, which is used for short-range potentials.

In the case of molecular solutions, unlike simple liquids, it is impossible to relate unambiguously the behaviour of the atom–atom potential to the type of closure; therefore, the closure conditions for the atom–atom functions are not rigorously deduced but are also expressed in the HC or PY approximation. This idea has been developed extensively in the Reference Interaction Site Model (RISM) theory,[90] in which the CF are related by the integral relations

$$\rho \boldsymbol{H}_{AB}(R) = \sum_{CD} \boldsymbol{W}_{AC}(r) C_{CD}(\boldsymbol{r} - \boldsymbol{r}_1) \boldsymbol{X}_{DB}(|\boldsymbol{r}_1 - \boldsymbol{R}|) \mathrm{d}\boldsymbol{r} \mathrm{d}\boldsymbol{r}_1. \qquad (20)$$

Here ρ is the average density of the solvent; H and C are matrices whose elements are the h_{AB} and c_{AB} functions for atoms of different types, respectively; C and D are additional subscripts for the solute and solvent atoms, respectively; $\boldsymbol{W}_{AC}$ is the 'structural matrix' composed of the solute correlation functions w_{AC}, and

$$\boldsymbol{X}_{DB}(r) = \boldsymbol{W}_{DB}(r) + \rho \boldsymbol{H}_{DB}(r) \qquad (21)$$

is the generalised susceptibility of the pure solvent. Here, matrices are introduced instead of three scalar integral equations for the solute–solute, solute–solvent and solvent–solvent correlation functions. The $\boldsymbol{X}_{DB}$ matrix can be calculated by the MC or MD methods or using integral equations. Like the structural matrix for the complex solute $\boldsymbol{W}_{AD}$, this matrix specifies the input structural data for Eqn (20). As regards the mathematical statement, the equations of the RISM theory are similar to Eqn (19) and differ only by the presence of an additional weighting factor $\boldsymbol{W}$ caused by intramolecular bonds. The large number of discrepancies between the asymptotic estimates of various physical properties and the conclusions drawn in terms of the RISM models are due to the approximate character of this analogy.[86,91] In particular, for polar liquids, the RISM model substantially underestimates the dielectric constant and, for example, for water, it does not predict adequately thermodynamic and structural properties.[92] More rigorous approaches also exist;[93] however, these are seldom used to study solvation due to the complexity of numerical implementation.[94]

As noted above, all the thermodynamic characteristics of solvation can be found in terms of the AACF. The form of the relevant relations depends on the type of closure. The simplest relations are obtained in the case of the HC approximation where the excess chemical potential μ in the limit of an infinitely dilute solution is determined from the equation [95]

$$\beta\mu = \rho \sum_{AB} \int \left[\frac{1}{2} h_{AB}^2(r) - c_{AB}(r) - \right. \qquad (22)$$

$$\left. - \frac{1}{2} \sum_{CD} \int c_{AC}(r) X_{CD}(|\boldsymbol{r}_1 - \boldsymbol{R}|) c_{DB}(r)(|\boldsymbol{r} - \boldsymbol{r}_1|) \right] \mathrm{d}\boldsymbol{r} \mathrm{d}\boldsymbol{r}_1.$$

By using standard thermodynamic relations, one can also calculate the energy E, the enthalpy H and the entropy Γ of solvation [96]

$$E = \left. \frac{\partial(\beta\mu)}{\partial\beta} \right|_{\rho}, \qquad (23)$$

$$H = \left. \frac{\partial(\beta\mu)}{\partial\beta} \right|_{P},$$

$$\Gamma = \frac{\mu - H}{T}.$$

The subscripts $|_{\rho}$ and $|_{P}$ mean that the derivatives are calculated at a constant density and pressure, respectively.

The RISM equations with allowance for closure, like Eqn (19), are heterogeneous Fredholm integral equations of the second kind in the unknown function $\gamma_{AB}(r)$. The numerical investigation is done using iterative methods. First, some indirect correlation function $\gamma^{in}(r)$ is specified. Then the $c_{AB}(r)$ function is determined using the closure conditions. For the resulting function, the Fourier transform is found and used in the integral equation written in the k space for the calculation of the $\gamma_{AB}(k)$ function. The Fourier inversion is performed for the $\gamma^{out}(k)$ function found, and the process is repeated once again. The procedure of convergence can be accelerated by using various algorithms based on the Newton–Raphson method.[97,98]

The integral equations can be analytically solved only for a very limited set of potentials and closures.[99] Despite the small number of such analytical solutions, they are useful for the modelling of structural and thermodynamic properties of solutions on the basis of simplified models. The most important example for polar liquids is represented by the Mean Spherical Approximation (MSA) in which the closure is described in the following form

$$h(r < d) = -1, \qquad (24)$$

$$c(r > d) = -\beta u(r)$$

where d is the diameter of the solid sphere.

With this closure, analytical solutions were obtained for solid spheres having an electric charge or a dipole moment.[100] The properties of the MSA allow one to obtain analytical expressions for the free energy of solvation and other thermodynamic values in ion–dipole systems.[101] The model can be successfully used to study solvation in water–salt solutions.

In recent years, new calculation schemes have been developed (Three-Dimensional Interaction-Site Model, 3DRISM) [102–108] in which the structure of the solvent near the solvated molecule is

† The function h is the full CF. From the standpoint of a mathematician, this function is more convenient, as $h(r \to \infty) \to 0$ and the integrals that include $h(r)$ are finite, while $g(r \to \infty) \to 1$. In addition to these CF, the 'indirect' CF is also used: $\gamma \equiv h - c$.

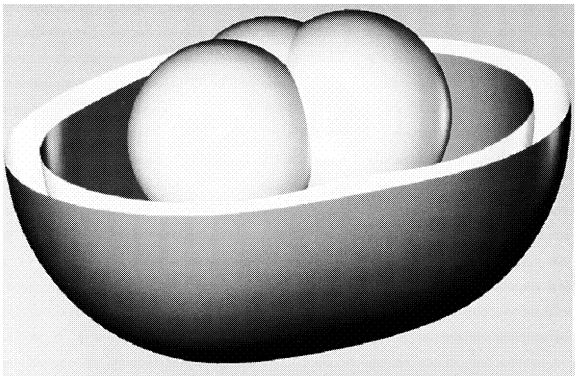


Figure 1. Isovalue surface of the propane – oxygen of the MACF $g(\boldsymbol{r}) = 1.5$ around the propane molecule.[102]

determined by the molecular – atomic correlation functions (MACF) $g_B(\boldsymbol{r})$. These functions characterise the probability that atom B of the solvent molecule is found at point $\boldsymbol{r}$, which is specified in the system of coordinates related to the solvated molecule. Figure 1 shows the sectional view of the MACF $g(\boldsymbol{r})$ isovalue surface for the propane molecule in water.[102] An equation similar to Eqn (20) can be written for MACF,

$$\rho h_B(\boldsymbol{r}) = \sum_A \int c_B(\boldsymbol{r}) X_{AB}(|\boldsymbol{r} - \boldsymbol{R}|) d\boldsymbol{R}, \quad (25)$$

where $c_B(\boldsymbol{r})$ is the 'direct' molecular – atomic CF. For $c_B(\boldsymbol{r})$, the HCA closure is constructed to relate $c_B(\boldsymbol{r})$ to $g_B(\boldsymbol{r})$. In fact, this assumes the additivity of action of the solvated molecule on separate atoms of the solvent molecule. Although $X_{AB}(\boldsymbol{r})$ is a radial function, the interaction potentials $u_B(\boldsymbol{r},\boldsymbol{\Omega})$ and $c_B(\boldsymbol{r},\boldsymbol{\Omega})$ depend, in the general case, not only on the distances but also on the orientation $\boldsymbol{\Omega}$ with respect to the solvated molecule. The relations involved in the 3DRISM model, unlike the integral equation (20), represent a set of three-dimensional integral equations. The algorithm for the solution of the 3DRISM equation is similar to that described above and differs only by the fact that it requires performing calculations on a three-dimensional network and using the three-dimensional Fourier transform in order to find $\gamma(k_x, k_y, k_z)$.

Yet another modification of the method of integral equations is the study of the molecular correlation functions (MCF) $g_{AB}(\boldsymbol{r},\boldsymbol{\Omega})$,[109,110] which depend on both the distance between the centres of the molecules and the relative angular orientation of molecules. A 'molecular' integral equation similar to Eqn (19) can be written for MCF

$$\gamma(\boldsymbol{r},\boldsymbol{\Omega}) = h(\boldsymbol{r},\boldsymbol{\Omega}) - c(\boldsymbol{r},\boldsymbol{\Omega}) = \quad (26)$$

$$= \rho \int h(\boldsymbol{r} - \boldsymbol{R},\boldsymbol{\Omega}_1) c(\boldsymbol{R},\boldsymbol{\Omega} - \boldsymbol{\Omega}_1) d\boldsymbol{R} d\boldsymbol{\Omega}_1 .$$

With this type of notation, one can avoid the problems caused by the choice of closure, because the diagram expansion method is naturally extended to the MCF. However, this gives rise to new problems associated with the increase in the dimension of integration in Eqn (26), which leads to a pronounced increase in the number of network points in the numerical approximation of the function $\gamma(\boldsymbol{r},\boldsymbol{\Omega})$. As a consequence, it becomes virtually impossible to find an analytical solution to Eqn (26). One way of avoiding the integration by angles is to expand the orientation-dependent CF into a series in eigenfunctions of the rotation operator $D^{mnl}_{\mu\lambda}(\Omega_1, \Omega_2, \Omega_R)$. The presence of a particular symmetry group for the solvent particles can reduce significantly the number of expansion terms. In some cases, rather fast convergence of the series ensures a good result even with a relatively small number of terms.[109] Comparison of these results with the results of MC

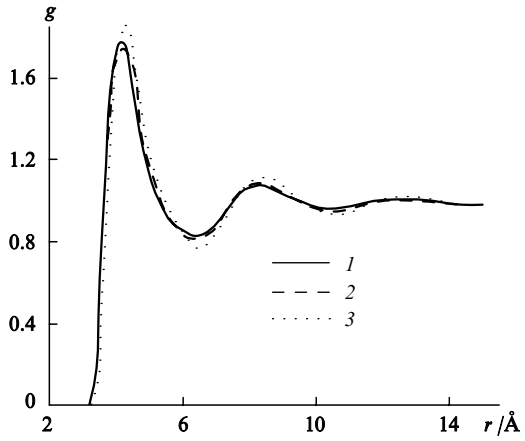


Figure 2. Carbon – methyl correlation functions for acetonitrile;[109] (*1*) solution of the molecular integral equations, (*2*) calculation using the RISM equations, (*3*) MC calculation.

calculations showed close agreement of the data for acetonitrile (Fig. 2). However, the scope of this approach is limited; it can be successfully used only for highly symmetrical solvated complexes.

The main difficulty involved in the use of the method of integral equations is the complexity of its numerical implementation on a computer. In each particular case, it requires designing of special subroutines for different types of closure, potentials, *etc.*; moreover, there is no assurance that the developed algorithm will ensure convergence of the iteration procedure. However, the method of integral equations has also a number of advantages over the MC and MD calculations. For equally complex systems, the amount of calculation is 2 to 3 orders of magnitude smaller in this method than in the two other methods. Since the correlations that are calculated are considered to decay rapidly with an increase in the distance between the particles, the method can be formulated for finite spatial areas. The method does not imply the choice of a periodic spatial cell during the modelling, and the results are not subject to the influence of the boundary conditions. Using modern versions of the method of integral equations, calculations of the solvation can be performed for macromolecules comprising up to 10^3 atoms. Owing to the possibility of renormalisation of the sought-for correlation functions, this method is also applicable to systems that are difficult to treat in terms of the MC or MD calculations. Examples are systems that incorporate solutes of complex shape or with a large electric charge, electrolyte solutions with low ion strengths, *etc.*

V. Electrostatic interactions in the Monte Carlo and molecular dynamics methods

The complexity of MC and MD calculations of the solvation in polar liquids is due to the fact that calculations are carried out for some limited volume of space (a cell); this may be associated with substantial errors due to the long-range character of the Coulomb forces. The use of periodic boundary conditions requires 'cutting off' the Coulomb potentials (usually, at a distance about half of the cell size). This distortion of the potential has only a weak influence on the radial dependence of the CF; however, it can change significantly the behaviour of the orientation correlations. The characteristics of cutting off the Coulomb potentials have been studied rather long ago. The interest in this effect was enhanced after publication of the paper [111] in which it was shown that this procedure gives rise to a false pattern of interaction of hydrated iron ions. With the cut-off Coulomb potential, likely charged ions were attracted at long distances, whereas calculation by the Ewald method [85] correctly predicted the asymptotic behaviour of the ions.

The Ewald and reactive field calculations are currently the best methods for taking into account the electrostatic interactions in solvation systems.[112–114] The Ewald method first developed for the calculation of Coulomb interactions in ion crystals[115] is considered to be the most consistent in the calculation of electrostatic potentials. In its modification for periodic molecular systems, the electrostatic energy (U) is expressed through the periodic Ewald pair potential $\varphi(\boldsymbol{R})$ (see Ref. 85)

$$U = \sum_{I<J}\sum_{\alpha\beta} q_{I\alpha}q_{J\beta}\varphi(|\boldsymbol{R}_{I\alpha} - \boldsymbol{R}_{J\beta}|) + \sum_{IJ}\sum_{\alpha<\beta} q_{I\alpha}q_{J\beta}\left[\varphi(|\boldsymbol{R}_{I\alpha} - \boldsymbol{R}_{J\beta}|) - \frac{1}{|\boldsymbol{R}_{I\alpha} - \boldsymbol{R}_{J\beta}|}\right] + \sum_{I\alpha}\frac{q_{I\alpha}}{2}\lim_{R\to 0}\left[\varphi(\boldsymbol{R}) - \frac{1}{|R|}\right]. \quad (27)$$

The subscripts α and β designate different atoms in different molecules I, J (of the solute or the solvent). The first two terms in this equation correspond to inter- and intramolecular electrostatic contributions to U. The last sum (this term is also called self-action) is a correction, which is necessary because in the point charge limit, the Ewald potential does not reproduce accurately enough the Coulomb potential within an area of the finite size. The sum of partial charges $q_{I\alpha}$ of all atoms disappears for electrically neutral systems. In this case, the use of the Ewald potential is the most justified. For charged solute–solvent systems, the self-action term turns into a constant which can be estimated from the condition

$$\lim_{R\to 0}\left[\varphi(\boldsymbol{R}) - \frac{1}{\boldsymbol{R}}\right] = \frac{\zeta}{L},$$

where ζ is a constant equal, for example, to ~ 2.837297 for a cubic cell, L is the linear size of the modelling cell. The appearance of the constant ζ dependent on the modelling conditions is a flaw of the Ewald calculations and the problem related to it is still debated.[116–121] However, for many applications, it is sufficient to calculate the energy U to within this constant.

The Ewald potential $\varphi(\boldsymbol{R})$ itself can be written down as a sum of two rapidly converging series

$$\varphi(\boldsymbol{R}) = \sum_n \frac{\operatorname{erfc}(\eta|\boldsymbol{R} - nL|)}{|\boldsymbol{R} + nL|} + \sum_k \frac{4\pi}{k^2L^3}\exp\left[-\frac{k^2}{4\eta^2} + ik\boldsymbol{R}\right] - \frac{\pi}{L^3\eta^2}, \quad (28)$$

where η is a shielding parameter which controls the convergence and the relative contributions of the series. However, formally, the Ewald potential does not depend on the selection of this parameter, *i.e.*,

$$\frac{\partial\varphi(\boldsymbol{R})}{\partial\eta} = 0,$$

while the cell-averaged value of this potential is also equal to zero

$$\int_{L^3}\varphi(\boldsymbol{R})\mathrm{d}\boldsymbol{R} = 0.$$

The difference between the Ewald potential and the reactive field potential (see below) is in the way the charge distribution which compensates the total charge of the solvation system is specified. In the case of the Ewald potential, this charge is uniformly distributed over the cell chosen for calculations, whereas in the reactive field method, it lies on a sphere with the radius R_c around the solvated ion under consideration. The calculations[85,116–118] showed that in practice, the Ewald potential approximates rather closely the electrostatic interaction.

In the reactive field method, the electrostatic interaction is approximated by using the potential[112–114]

$$\varphi(R < R_c) = \frac{1}{R} - \frac{1}{R_c} + \frac{(2\varepsilon_0 - 1)(R^2 - R_c^2)}{(2\varepsilon_0 + 1)R_c^3}, \quad (29)$$

$$\varphi(R > R_c) = 0.$$

The cut-off (at $R > R_c$) Coulomb interaction is modified by adding a surface field borrowed from the continuum theory. Actually, $\varphi(R)$ is the solution of the Poisson equation for the point charge located at the centre of a spherical cell with the size R_c immersed in a dielectric medium with the permeability ε_0 and the compensating surface charge on the cell surface. This approximation is used in the MD simulation of an ensemble of solvent molecules surrounding the solute.[21,22] In the calculation of the medium response field, the problem of finding the solvation energy is reduced to a hybrid computation (MD/CM) in which some of the molecules of the liquid (inside the chosen cell) are calculated (in the explicit form) by the MD method, while other molecules (outside the cell) are calculated using continuum models. Detailed description of the calculation algorithms on the basis of this hybrid discrete and continuum approach has been reported.[122] The researchers have found that this protocol allows one to calculate the electrostatic contributions to the free energy of solvation to an accuracy of several kilocalories per mole.

VI. Hydrophobic effects

Noble gases and hydrocarbons are typical examples of hydrophobic solutes. Their poor solubility in water is due to the entropy loss related to the entropy of hydration, which counterbalances or exceeds the benefit in enthalpy.[123] The main difference between the hydrophobic and hydrophilic solutes is the fact that the former have no charged or polar groups, which shows itself as the absence of electrostatic contributions to intermolecular potentials.

Study of the hydration of hydrophobic solutes is associated with two problems.[124] First, adequate simulation of hydrophobic effects requires detailed information on the microstructure and thermodynamic state of water. This information is used as the input data for calculating the hydration. Water has a number of abnormal properties compared to other polar liquids; therefore, in the simulation of hydrophobic solutes, the choice of the molecular model of water and the calculation of its properties should be carried out with special care. The microscopic models of water specially designed for this purpose allow one to calculate rather accurately the thermodynamic parameters of solvation for simple hydrophobic solutes.[125] Figure 3 shows the temperature dependences of the chemical potential (μ) and its enthalpy (h) and entropy (s) contributions for a methane molecule hydrated under atmospheric pressure. It can be seen that calculated and experimental data agree both qualitatively and quantitatively.

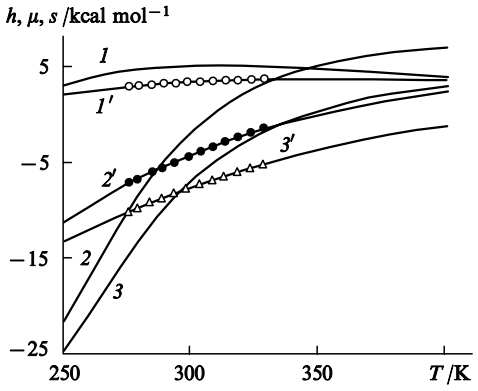


Figure 3. Temperature dependences of the chemical potential (*1*, *1′*) and its enthalpy (*2*, *2′*) and entropy (*3*, *3′*) contributions for a methane molecule hydrated under atmospheric pressure; (*1–3*) calculation,[125] (*1′–3′*) experiment.[126]

The second characteristic feature of hydrophobic solutes is related to geometric factors and excluded volume effects. Depending on the size of the solute, these effects can be manifested in different ways.[127] For small hydrophobic solutes (such as atoms of noble gases) at low concentrations, the packing effects are associated with reorganisation of water around the solute without rupture of a large number of hydrogen bonds. For mesoscopic hydrophobic solutes (for example, globular proteins), solvation can result in the cleavage of a large number of hydrogen bonds, giving rise to a nonwetting area near the hydrophobic surface of the solute where water occurs in the vapour state.

As an example, we shall consider a spherical model of the solute with a large radius R, which resides in the excluded volume cavity having the same radius. For macroscopically large cavities, Gibbs free energy of solvation is described by the expression [128, 129]

$$\Delta G \sim \frac{4\pi R^3 p}{3} + 4\pi\sigma R^2, \tag{30}$$

where p and σ are the hydrostatic pressure and the liquid – vapour surface tension coefficient, respectively.

By parametrisation,[130, 131] this relation can be extrapolated to microscopic cavities which arise upon solvation of molecular species. The first term in relation (30) becomes negligibly small at normal pressures, and the σ value remains the only significant parameter to determine ΔG. In early publications (see, for example, Ref. 128), this parameter has still been interpreted as macroscopic surface tension, although a consistent formulation [129] interprets σ as a model parameter dependent on the solvent and the cavity size and shape. This approach, called the scaled particle theory, was modified to be applied to non-spherical cavities.[132, 133] The modern version is based on the density functional theory,[127] where the free energy of solvation is expressed in terms of generalised water susceptibility $X(r, r')$ [see Eqn (21)]. The free energy of cavity formation in the solvent is called the cavitation energy. It is mainly of the entropy nature. In the absence of electrostatic interactions, the total energy of solvation consists of the cavitation and van der Waals contributions. The latter contribution is due to short-range interactions (which are usually described using Lennard-Jones parametrisation) and is largely an enthalpy effect. The peculiarity of the situation is that the cavitation and van der Waals contributions have opposite signs (Fig. 4). The magnitude of each contribution grows with an increase in the size of the cavity [134] (often, they are regarded as being proportional to the surface area of the cavity [135]), whereas the overall effect is small ($\sim 2-3$ kcal mol^{-1}) and barely depends on the size of the cavity (at least, for hydrocarbons with a number of carbon atoms ranging from 1 to 6).

Yet another molecular model of the hydrophobic effect is formulated on the basis of the Pratt and Chandler theory [136] in terms of the integral equation method. This theory reduces determination of ΔG to the calculation of the AACF. It is closely related to the most developed molecular model of hydrophobic solvation, based on the information theory [124, 137] and is actually a cavitation effect model. With this approach, the free energy of solvation ΔG of a non-polar solid particle is determined in terms of the probability p_0 of formation of a cavity with the corresponding size and shape in the bulk of the liquid

$$\beta\Delta G = -\ln p_0. \tag{31}$$

The probability p_0 can be found by computer simulation [138–150] or in terms of many-particle correlation functions.[130] The following simple procedure is also efficient.[149–152] One should consider the probability distribution $\{p_n\}$ for which the case $n = 0$ corresponds to the probability of formation of an excluded volume cavity [see Eqn (31)]. The p_n values for $n \neq 0$ are interpreted as the probabilities that n solvent (water) molecules are situated in the cavity. The zero, first and second probability moments $\{p_n\}$

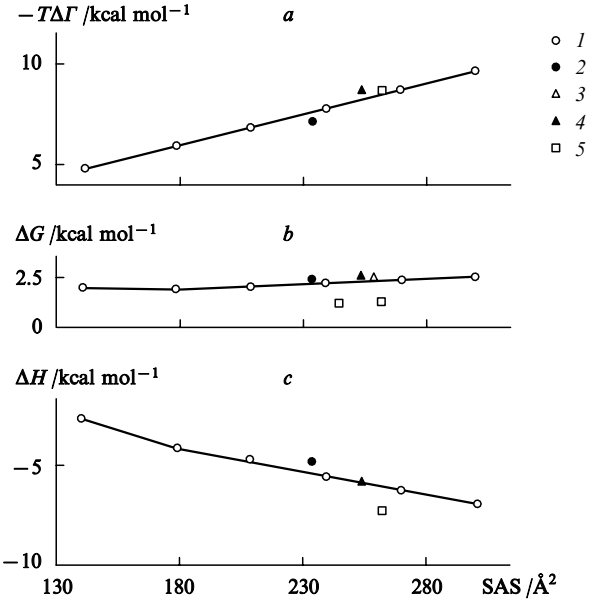


Figure 4. Experimental values of the entropy (*a*), free energy (*b*) and enthalpy (*c*) contributions to the hydration of isobutane (*1*), 2-methylbutane (*2*), neopentane (*3*), cyclopentane (*4*) and cyclohexane (*5*); the line shows the approximation of the discrete values by some dependence.[134]

$$\langle 1 \rangle = \sum_n p_n ,$$

$$\langle n \rangle = \sum_n n p_n ,$$

$$\langle n^2 \rangle = \sum_n n^2 p_n ,$$

respectively, can be expressed in terms of values that can be measured experimentally, namely, the density and the generalised susceptibility of water. The distribution $\{p_n\}$ is simulated in the form

$$p_n = p_{0n} \exp(\lambda_0 + \lambda_1 n + \lambda_2 n^2), \tag{32}$$

where p_{0n} is the simplest 'primer' distribution, $p_{0n}(n < n_{\max}) = \text{const}$ and $p_{0n}(n > n_{\max}) = 0$, where the maximum number of particles in the cavity $n_{\max}$ is the distribution parameter.[145] The additional parameters, $\lambda_0, \lambda_1, \lambda_2$, are found from the condition of reproducing the three first probability moments $\{p_n\}$, which are specified as noted above. Expression (32) corresponds to the maximum of informational entropy with additional constraints imposed on the moments.[149] By constructing the entropy functional in such a way that the zero, first and second probability moments corresponded to experimental data, Vener *et al.*[122] have found an expression for the free energy of hydration of noble gas atoms

$$\beta\Delta G \approx \frac{\rho^2 \upsilon^2}{\delta n^2}, \tag{33}$$

where ρ is the density of solvent (water) particles, υ is the volume of the excluded volume cavity, $\rho\upsilon = \langle n \rangle$ is the average number of solvent particles in the cavity, $\delta n^2 = \langle n^2 \rangle - \langle n \rangle^2$ is the variance of the number of particles in the cavity. According to this approximate relation, the temperature dependence of the cavitation energy is determined by two factors, namely, the dependences $\langle n \rangle(T)$ and $\delta n^2(T)$. Relation (33) was confirmed by computer simulation of small-sized solutes;[124] however, the result is deteriorated with an increase in the size of the excluded volume cavity,[134] apparently, due to the excessively simplified ('planar') form of the function p_{0n}, chosen according to Eqn (32). The MC-

and MD-based simulation shows that, generally, the theory described above reproduces qualitatively the hydrophobic effect but does not provide a quantitative estimate of the temperature dependence of cavitation free energy for solutes of an arbitrary size.

Direct MD and MC calculations of thermodynamic functions are complicated and cumbersome. There are several algorithms efficient for the calculation of free energy, namely, the Umbrella Sampling, Thermodynamic Perturbation, and Thermodynamic Integration methods.[16, 139–141] The last two methods are used most often; they are useful for the calculation of cavitation effects.[134, 146] They differ only in procedural points and give the required result after a sequence of consecutive standard MC or MD calculations.

Let us consider, as an example, the use of thermodynamic integration for determining the change $\Delta G = \Delta G_{XY}$ of the free energy of a solvation system

$$G = \beta^{-1}\langle \exp(-\beta U)\rangle$$

caused by its transition from the initial state X to the final state Y upon transfer of a solute particle from the gas phase to the solution. Here U is the potential energy of interactions between the solute and solvent particles and interactions of solvent particles with one another. This value is regarded as a function of the coordinates of solvent particles. Averaging $\langle ... \rangle$ should be carried out over an equilibrium ensemble of solvent configurations in the presence (Y) and in the absence of the solute (X). To carry out this calculation, an additional parameter λ, equal to zero in the state X and equal to unity in the state Y, is introduced in the potential U. This parameter acquires discrete values $\lambda_i = 0, \lambda_1, \lambda_2, \ldots, \lambda_i, \ldots, 1$ in the segment (0,1). Thus the change in the free energy ΔG can be calculated as follows

$$\Delta G = -\frac{1}{\beta}\sum_i \ln\left\langle \exp\{-\beta[U(\lambda_{i+1}) - U(\lambda_i)]\}\right\rangle_{\lambda_i} = \int_0^1 \left\langle \frac{\partial U(\lambda)}{\partial \lambda}\right\rangle_\lambda d\lambda, \quad (34)$$

where $U(\lambda)$ is the potential considered as a function of λ. Analogous relations can be obtained for the enthalpy and entropy contributions to ΔG. The change in the entropy $\Delta\Gamma$ is determined by the formula

$$-\Delta\Gamma = \beta\int_0^1 \left[\left\langle U(\lambda)\frac{\partial U(\lambda)}{\partial\lambda}\right\rangle_\lambda - \langle U(\lambda)\rangle_\lambda \left\langle \frac{\partial U(\lambda)}{\partial\lambda}\right\rangle_\lambda\right] d\lambda. \quad (35)$$

Thus, calculation of thermodynamic values includes a series of MC or MD computations with fixed λ_i followed by numerical integration according to Eqn (34) or (35). The values of the parameter λ can be varied not only by deterministic choice of the intermediate λ_i values but also in a stochastic way during the solution of MD equations [153, 154] in which the variable λ is included as an additional degree of freedom.

The above-described thermodynamic integration method has been used to study the temperature dependence of the thermodynamic characteristics of the hydration of hydrocarbons.[143, 144, 155] The functional dependence of the binding energy on the distance between the solute and solvent molecules has also been studied.[156, 157] Computations performed by various researchers have now been reported [134, 155, 158] where thermodynamic perturbation and thermodynamic integration procedures have been used for systematic study of the changes in the free energy, the enthalpy and the entropy upon hydration of lower alkanes containing one to six carbon atoms. The results of these calculations were compared with experimental results. However, it was found that the results of MC and MD computations can deviate from experimental thermodynamic data (Table 2), although generally they provide an adequate estimate of the relative changes in ΔG. For hydrophobic molecular solutes, the results of calculations can be substantially improved by using the 3DRISM procedure and an additional empirical calibration of closure conditions.[104]

Table 2. Experimental and calculated [by 3DRISM, XSOL (Extended Solvation), SMx, SCF and MC methods] values of free energy of hydration ΔG (kcal mol^{-1}) for various solutes.

Solute	Experiment (see [54])	Calculation by the method				
		3DRISM (see [104])	XSOL (see [159])	SMx (see [160])	SCF (see [50])	MC (see [11])
CH_4	2.0	2.084	4.5	2.0	–	–
C_2H_6	1.83	1.827	4.1	1.2	–	2.5
n-C_3H_8	1.96	2.024	–	–	–	–
n-C_4H_{10}	2.08	2.136	–	–	–	–
n-C_5H_{12}	2.33	2.292	–	–	–	–
C_6H_6	−0.8	–	−0.7	−1.0	−0.8	−2.9
$C_6H_5CH_3$	−0.8	–	−1.7	−0.9	−0.8	–
CH_3OH	−5.1	−3.634	−4.0	−5.4	−5.2	−5.1
C_2H_5OH	−5.0	−3.375	−5.5	−4.9	−4.5	–
iso-C_3H_7OH	−4.8	−2.939	−4.0	−3.8	−4.4	–
C_6H_5OH	−6.6	–	−7.5	−6.6	−5.9	–
H_2O	−6.3	–	−7.7	−9.5	−7.3	–
CH_3OCH_3	−1.9	–	−0.5	−2.4	–	−2.6
CH_3COCH_3	−3.8	–	−1.7	−4.3	−4.5	−3.6
CH_3CO_2H	−6.7	–	−6.7	−6.5	−7.3	−7.7
$CH_3CO_2CH_3$	−3.3	–	−4.1	−4.0	–	−4.6
CH_3CN	−3.9	–	0.8	−4.3	–	−5.0
CH_3NH_2	−4.6	–	−4.4	−5.8	−4.3	−6.5
$C_2H_5NH_2$	−4.5	–	−3.2	−4.7	−4.7	–
CH_3CONH_2	−9.7	–	−7.2	−10.3	−11.0	−11.9
(*Z*)-NMA	−10.1	−6.236	−10.0	−7.8	−8.7	–
(*E*)-NMA	−10.1	−6.874	−10.4	−7.3	−9.0	–
C_5H_5N	−4.7	–	−4.5	−5.0	–	−5.1
4-MeC_5H_4N	−4.9	–	−4.8	−4.9	−5.1	–

To conclude the Section, we would like to note that, despite the many years of investigation of hydrophobic effects and the advances made due to the development of molecular models for the hydrophobicity phenomenon,[124, 127, 129–136] the theory is still far from being completed because in the general case, hydrophobic behaviour is due not only to the type of interaction potentials or the solute geometry, but also to collective effects related to the entropy factor.[161]

VII. Solvation of ions

Solvation of ions is a trial for various molecular models, as it allows one to reveal the scope and drawbacks of one or another approach. The classical MC and MD models of solvation of monoatomic ions, as well as molecular solutes, make it possible to calculate the microstructure of the solvent around the ion; however, in the case of solvation energy, agreement with the experimental results is less satisfactory. Even accurate MD calculations based on the Ewald potential give deviations of up to 20% of the experimental values.[162] Therefore, in recent years, calculations based on either hybrid and combined protocols (Table 3) or classical polarisation models have been actively carried out. In these procedures, the calculation of the solvation of monoatomic ions is a test routine for verification of the calculation scheme. The quantum corrections usually result in smoother AACF and smaller coordination numbers of the solvated ion (Fig. 5). Quantum calculations also give lower potential barriers for proton or electron transfer. This is clearly seen in relation to the hydrated proton (Fig. 6).

The spherical symmetry of monoatomic ions allows one to derive analytical expressions for the solvation energy within the bounds of different models of the medium. Comparison of these expressions clearly demonstrated the influence of the structure of

Table 3. Experimental and calculated thermodynamic characteristics of hydration (kcal mol^{-1}) of various ions.

Value	Method	Na^+	K^+	F^-	Cl^-	Ref.
ΔE	XRISM [a]	0.10	−0.60	2.17	−0.20	163
	experiment	0.25	−0.25	–	−0.27	164
$-\Delta G$	XRISM [a]	80.04	62.01	148.1	86.6	165
	XRISM [a]	77.3, 84.0	65.6 –	– –	83.9, 81.9	96, 108
	3DRISM	80.1			79.5	108
	MC	94.8	64.5	138	88.3	162
	SM5	–	–	106.9	77.3	161
	MD/CM	104.5	75.2	129.1	80.1	122
	QM/MM	–	–	109	81	163
	experiment	89.6, 96.4	72.7, 78.9	110	80.5, 73.9	166, 167
$-E$	XRISM [a]	89.05	71.49	168.8	101.5	164
	XRISM [a]	88.8, 93.7	75.8	–	101.1, 96.7	96, 108
	3DRISM	90.2	–	–	93.5	108
$-H$	XRISM [a]	94.1, 93.6	75.0		105.7, 94.1	96, 108
	3DRISM	95.6	–		98.9	108
	experiment	99.9, 106.6	80.3, 86.6		88.2, 81.8	166, 167

[a] Extended Reference Interaction Site Model.

the solvent on the solvation effects. Let us consider particular examples of the calculation of free energy of solvation of an ion with the charge Q in a spherical cavity with the radius a.

According to Born,[4] the medium around the cavity is characterised by an invariable dielectric constant, ε_0, while the free energy of solvation is determined by the following relation:

$$\Delta G = -\frac{Q^2}{2a}\left(1-\frac{1}{\varepsilon_0}\right). \tag{36}$$

In this equation, the cavity radius a should be considered as some effective value. Direct use of crystallographic ionic radii gives unsatisfactory results. It has been shown [170] that for ions

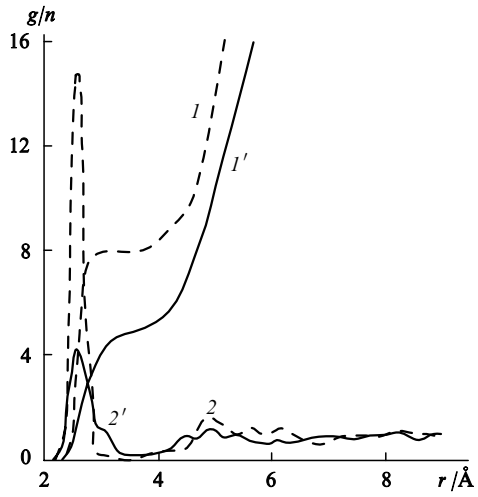


Figure 5. Dependences of the atom–atom (Na–Na) correlation function g (*1*, *1′*) and the coordination number n (*2*, *2′*) on the distance between the centres of the sodium ions solvated in ammonia.[168]
The dashed line corresponds to the classical MD calculation and the continuous line shows the QM/MM calculation.

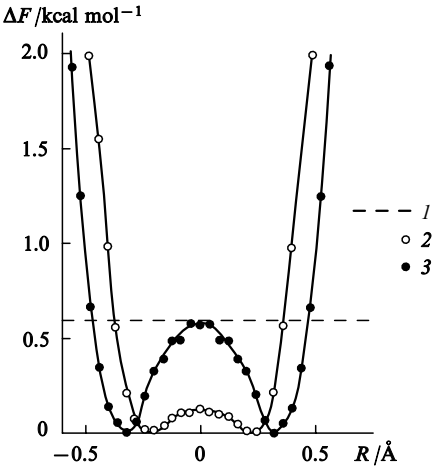


Figure 6. Free energy ΔF of the hydrated proton *vs.* its coordinate R relative to the midpoint of the O–O bond.[169]
(*1*) energy at 300 K, (*2*) QM calculation, (*3*) MD calculation.

with a rather large size, relation (22) is converted into the Born formula with $a = r_{max}$, where r_{max} is the distance from the ion centre to the first maximum of the radial distribution function $g(r)$. The difference between the values of free energy of hydration of spherical ions found using the Born approximation and by direct solution of the RISM equations for Cl^+ and Cl^- ions is less than 12%.[160] By applying various corrections to formula (36), one can attain a satisfactory agreement between the calculation data and experimental results for a large number of monoatomic ions.[50, 160, 171] The situation regarding the separation of the enthalpy ΔH and entropy $T\Delta\Gamma$ contributions to the Gibbs free energy

$$\Delta G = \Delta H - T\Delta\Gamma. \tag{37}$$

is less successful.

Even in complex calculations of the solvation effects, the use of experimental data on the temperature and pressure dependences of the dielectric constant $\varepsilon_0(T,P)$ makes it possible to reach quantitative agreement with experimental thermodynamic data (see Table 3).

Direct MD and MC calculations for the free energies of solvation of polyatomic ions with non-spherical shapes have been reported.[12, 172, 173] Successful implementation of these calculations requires that thorough parametrisation of the Lennard-Jones interaction between atoms of the solute and solvent particles be carried out. Apparently, the dependence of this parametrisation on the partial electric charge on atoms of the ionic solute should also be carried out.[174] However, the problem of selection of appropriate parameters is appreciably complicated by great scatter of experimental data obtained by different researchers for ionic systems.

For qualitative understanding of the solvation effects at the molecular level, it is expedient to continue with the discussion of the solvation models of spherical ions. In doing this, one can see that explicit allowance made for the molecular structure of the solvent changes the theoretical views on the free energy of solvation.

Figure 7 shows the scheme of the concentric two-sphere model of solvation.[175–177] Inside a cavity with the radius a_1, the dielectric constant is equal to unity, while in the outer region, outside the sphere with the radius a_2, the dielectric constant is determined by the solvent and is equal to ε_0. The intermediate space between the inner and outer boundaries contains a layer with ε_∞ (the optical dielectric constant). For this model, the free energy of solvation is equal to

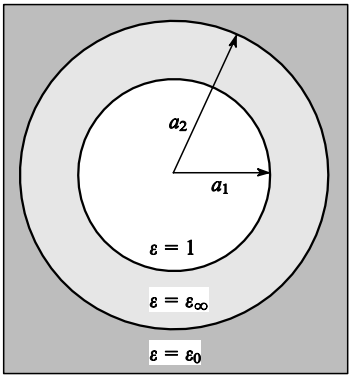


Figure 7. Scheme of the two-sphere model of solvation.

$$\Delta G = -\frac{Q^2}{2}\left[\left(1-\frac{1}{\varepsilon_\infty}\right)\frac{1}{a_1}+C\frac{1}{a_2}\right], \tag{38}$$

where C is the Pekar factor,

$$C = \frac{1}{\varepsilon_\infty}-\frac{1}{\varepsilon_0}. \tag{39}$$

In the non-local extension of the Born model, the dielectric constant is specified by the function $\varepsilon(k)$. In this case, the following approximate relation holds:[24–29]

$$\Delta G = -\frac{Q^2}{\pi}\int_0^\infty \mathrm{d}k\,\frac{\sin^2 ka}{k^2a^2}\left[1-\frac{1}{\varepsilon(k)}\right], \tag{40}$$

while for the simple Lorentzian model of the dielectric function $\chi(\boldsymbol{k})$ [see Eqn (10)] with $\chi_0 = (1-\varepsilon_\infty^{-1})/4\pi$, the following exact expression has been derived:[31]

$$\Delta G = -\frac{Q^2}{2}\left(1-\frac{1}{\varepsilon_\infty}\right) - \tag{41}$$

$$-\frac{CQ^2}{2}\,\frac{1+\sqrt{\varepsilon_0/\varepsilon_\infty}\,[\coth(a/\varsigma)-\varsigma/a]}{1+\sqrt{\varepsilon_0/\varepsilon_\infty}\,[\coth(a/\varsigma)-\varsigma/a]+\sqrt{\varepsilon_\infty/\varepsilon_0}(\varsigma/a)}.$$

In the MSA theory, according to which the solvent molecules are modelled as hard spheres with dipole moment m, the free energy of solvation is given by[101,178]

$$\Delta G = -\left(1-\frac{1}{\varepsilon_0}\right)\frac{Q^2}{2a+\varsigma}, \tag{42}$$

where a is the effective radius of the solute, ς is the correction to radius a, which depends on the temperature and is expressed in terms of m or ε_0 as the solution of the non-linear Wertheim equation.[179]

Relations (38)–(42) clearly demonstrate the influence of the solvent structure. In particular, in the last three models, the expression for the free energy of solvation is reduced to the Born formula (36) in the limit where the characteristic size of the solvent particles (the correlation length in the non-local models or the radius ς in the MSA model) is much smaller than the radius of the solvated ion. The opposite limit is also of certain interest. Detailed discussion of these asymptotic expressions and their comparison with experiment have been reported[176,177,180,181] and supplemented by qualitative interpretation on the basis of molecular modelling.[182,183]

The solvation of polyatomic ions is also studied on the basis of integral equations using the RISM method. The calculations based on the molecular integral equations (25) are laborious and it was not until recently that they started to be actively used to study the solvation of polyatomic ions.[184] Note that even for an infinitely dilute solution, the standard RISM model should be modified for well-posed allowance for the dielectric shielding effects, because it results in a false estimate of the dielectric constant of the solvent. To eliminate this drawback, in the XRISM model,[185] it is proposed to renormalise the Coulomb interaction of ions in solution assuming that

$$u_c(r_{AB}) = \frac{Aq_Aq_B}{r_{AB}}.$$

Here, the constant A is selected in such a way as to provide finally the required dielectric constant ε_0. In practice, the constant A is determined from experimental data. Usually, it differs little from unity (for water, $A \simeq 0.98$), and this modification of the Coulomb potentials has only a slight influence on the thermodynamic parameters of the liquid. The XRISM calculations of the hydration of various ions provide qualitative agreement between the theory and experiment (see Table 3). Generally, these calculations give reliable information concerning various structural characteristics of hydrated ions. The activation energy ΔE for transfer of a water molecule from the region near the ion to the region of pure solvent has been calculated.[163] These data are consistent with experiment.[164]

In the case of finite concentrations of solvated ions, the standard RISM and XRISM models lead to incorrect results, because the approximation of the linear response of the system to the external field created by a solvated molecule is violated. At low concentrations of ions, the plasma parameter

$$\zeta = \frac{l_B}{r_D}$$

[$l_B = e^2/(\varepsilon k_B T)$ is the Bjerrum length, r_D is the Debye radius] is small and the linear response approximation is plausible. However, at high concentrations of solvated ions, the plasma parameter is no longer small (for NaCl concentrations of about 0.05 mol litre^{-1} in water, $\zeta \simeq 0.5$). Hence, the ion-induced potential does not follow a linear dependence on the ion concentration and cannot be taken into account by mere renormalisation of the Coulomb interaction. For this case, the DRISM (Dielectric RISM) model has been developed;[186] in this model, the dielectric constant is included in the closure equation as the initial data. The calculations carried out using this model make it possible to estimate rather adequately the free energy and the salting-out coefficients for various concentrated salts.[187] It is noteworthy that DRISM calculations are needed in those cases where microscopic changes in the interaction of ions with a solvated macromolecule give rise to conformational rearrangements in the molecule, which involve rather large space.

In recent years, attempts have been made to use the 3DRISM models[104,107] or the method of molecular integral equations[188] to take into account the effect of the orientational correlations on the solvent structure near a polyatomic ion. Figure 8 shows the local structure of water around the Na^+-Na^+ ion pair calculated in terms of the 3DRISM model.[189] The deviation of the results obtained on the basis of this model from the results of MC and MD calculations is insignificant. Apparently, more accurate calculations could be carried out with appropriate calibration of the interaction potentials. Yet another promising route is to take into account the changes in the electronic structure of solvated ions caused by interaction with the solvent.

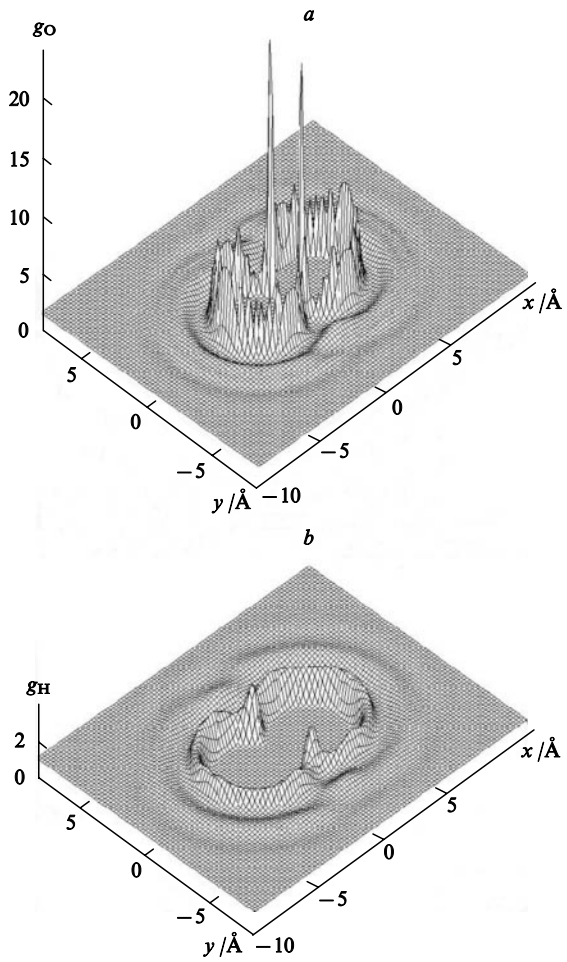


Figure 8. Molecule – atom ion – oxygen (*a*) and ion – hydrogen (*b*) correlation functions for the $Na^+ - Na^+$ pair in water.[189]
The *x*, *y*, *z* coordinates of the sodium ions are ±2.05, 0 and 0, respectively.

VIII. Polar molecules

The calculations of solvation for polar molecules are carried out in the same way as for ions. In the case of polar solutes, the effects of cutting-off the Coulomb interactions are usually neglected on the ground that the resultant electric field decays rather rapidly for these systems, *i.e.*, its potential

$$\varphi(R \to \infty) \propto R^{-n}, \quad n \geqslant 3,$$

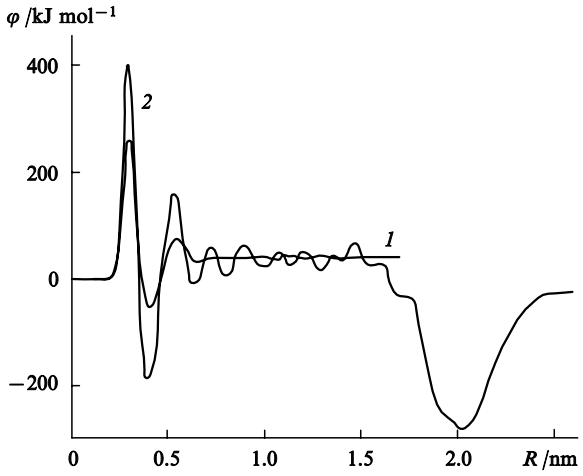


Figure 9. Electrostatic potential φ near the polar solute in water.[85]
(*1*) calculation by the Ewald method, (*2*) calculation for the cluster of 1024 water molecules by the standard MD method.

and the errors caused by the cutting-off effects are insignificant. However, accurate calculations for polarisable solutes[190] have shown that the way of cutting-off the potential $\varphi(\boldsymbol{R})$ still influences, although to a lesser extent, the induced charge of the solvent molecule and, hence, the calculated thermodynamic and structural properties of the system. Figure 9 shows the electrostatic potential around a polar solute in water.[85]

The modern trends in such studies take into account the many-particle interactions caused by the solute-induced polarisation of the solvent and turn to polarisable models of polar liquids (see, for example, Refs 191 – 193). These models (unlike non-polarisable ones) permit well-posed simulation of various processes in biological systems: electron transfer, solvatochromic changes of the electronic and vibronic spectra, *etc*. The results of computation of various characteristics of water in terms of polarisable and non-polarisable models of the solute and those found experimentally are summarised in Table 4. Richardi *et al.*[188] carried out computations within the framework of the same molecular model of water but on the basis of different methods. It can be seen that approximation (29) simulates rather closely statistic and dynamic characteristics of liquid water; the calculation of pressure is faced with difficulties because this value is determined by the balance of repulsion and attraction forces between molecules and is sensitive to the way of cutting-off the Coulomb potentials.

Currently, the most reliable estimates of the free energy of solvation of polar molecules are based on continuum models. Comparison of the theoretical and experimental data has shown

Table 4. Calculated and experimental values for the internal energy (U), pressure (P), dipole moment of the molecule (m), self-diffusion coefficient (D), relaxation time in the NMR method (τ_{NMR}), density (ρ) and dielectric constants (ε_0, ε_∞) of water.

U /kcal mol^{-1}	P /kbar	m /D	$10^{-9}\,D$ /m^2 s^{-1}	τ_{NMR} /ns	ρ /g cm^{-3}	ε_0	ε_∞	Ref.
Calculation methods								
−9.86	0.02	2.62	2.0 ± 0.03	2.2	–	–	–	190 [a]
−10.21	−0.7	2.66	1.5 ± 0.01	2.8	–	–	–	190 [b]
−9.92	−2.9	2.62	1.8 ± 0.03	2.1	–	–	–	190 [c]
−9.92	–	2.712	1.81 ± 0.06	2.6	0.997	98 ± 8	1.689	193
−9.89	–	2.6	1.9 ± 0.1	2.1	1.014	79 ± 8	1.592	194
−9.87	–	2.29	2.62 ± 0.04	1.4	0.999	82 ± 2	1.0	195
−10.40	–	3.01	–	–	1.02	–	–	196
Experiment								
−9.92	–	–	2.3	2.1	0.997	78.3	1.79	197 – 201

[a] Calculation in terms of the Ewald method. [b] Calculation using the cut-off Coulomb potential. [c] Calculation using the reactive field method.

that the difference between these values does not exceed 20%. This result is attained due to thorough parametrisation of models. However, at present, the continuum approaches tend to be upgraded, the modern phase in the modelling of solvation being characterised by active use of hybrid schemes. These schemes may include QM/MM computations [202] or the calculations in which some of the water molecules are explicitly taken into account, while other water molecules are taken into account in terms of a continuum approach.[203] The results point to a higher efficiency of hybrid procedures compared to the conventional procedures of the continuum theory (see Table 2). For instance, calculations of the solvation of the $Cl^+\cdots Cl^-$ complex based on a hybrid MD/CM model made it possible to estimate the electrostatic contribution to the free energy of solvation to within 1 kcal mol^{-1} (see Ref. 122).

General equation (34) of the thermodynamic integration method can be regarded as an estimate for the change in the free energy related to the transition of the solvation system from one state to another; this change is described by the parameter λ. The selection of λ is rather free. It can be described as a multidimensional vector whose components correspond to different contributions to the free energy of the system. With this interpretation, thermodynamic integration is widely used for estimating the role of Coulomb contributions to the free energy of solvation (see, for example, Refs 83, 85). It can also be applied for estimating the changes in the free energy caused by quantum effects. For example, this procedure has been used [204] to assess the quantum corrections to ΔG_s relying on the data of classical modelling as the initial conditions.

The method of integral equations also allows one to calculate the structural characteristics of solvation of polar molecules; however, the accuracy of the results obtained using the standard integral equations described above is much lower than in the MC or MD computations. This drawback is partially compensated by the relative ease of calculation of the solvation of large biomacromolecules. Thus for a fixed double helix conformation, RISM computations of hydration of a DNA fragment composed of 315 atoms [205] and a mellitin molecule containing 436 atoms have been carried out.[206] A calbindin molecule containing 722 atoms has been considered in a similar way.[207] In the general case, the conformation of a biomacromolecule can be found by a self-consistent procedure based on hybrid calculations of the IMCF by the MC method and numerical solution of the RISM equations.[208–211] At present, such calculations are carried out for peptides containing $\sim$ 20 to 200 atoms. Figure 10 shows one of the conformations found for the hydrated C-peptide of ribonuclease A.[211]

Yet another version of hybrid calculations are those done for solvated molecules in which the electronic structure of the solute is calculated by quantum chemistry techniques, while the spatial structure of the solvent is determined by the method of integral equations.[212–220] Table 2 shows the results of calculations of ΔG_s on the basis of SCF–RISM computations (XSOL).[159] In this case, as in MC calculations, only qualitative agreement with experimental data is attained. As noted above, this is due to an ill-posed allowance made for the molecular orientations in the standard RISM procedure. Apparently, the results could be markedly improved by using the 3DRISM model or by solving the molecular integral equations. The conduction of such hybrid calculations has started only recently.[217, 218]

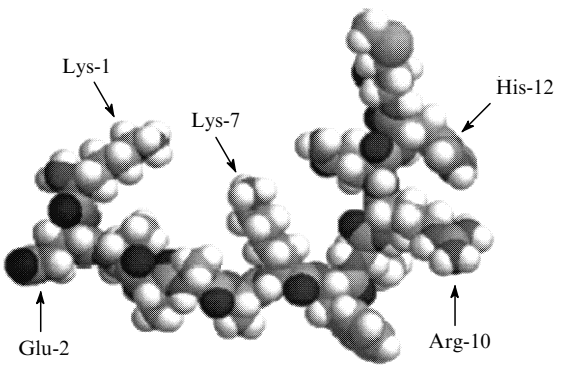


Figure 10. The most favourable conformation of C-peptide in aqueous solution.[211]
The arrows mark amino acids.

IX. Solvated quantum particles

In a study of solvation of a light quantum particle, an excess electron is considered most often. The interest in this type of studies is caused by two factors. First, such a quantum-and-classical hybrid system is convenient for demonstrating the potential of various hybrid schemes. Second, development of experimental procedures and the large amount of accumulated data on the behaviour of solvated electron (e_s) in various media [221] resulted in considering e_s as a unique test particle for testing the solution microstructure.

Early investigations of the solvated electron were based on the continuum approach;[222] it was assumed that e_s exists in a cavity surrounded by a dielectric medium with the constant ε. With this definition, the problem was reduced to the solution of the Schrödinger equation in the self-consistent field V_{ef} for the single-electron wave function $\phi(r)$. An alternative approach is to calculate the e_s characteristics on the basis of methods of the MC [223–226] or MD quantum model (QMD).[227–233] The application of these methods is based on the fact that the problem of the behaviour of a quantum particle in a liquid can be reduced to the equivalent problem of calculation of a classical polymer chain.[234] A large number of calculations for the solvated electron in water,[227] ammonia [223] and metal–ammonia solutions [235] have been reported. The results obtained are in good agreement with one another and correspond to experimental estimates. The modern studies also include SCF calculations, which take into account the discrete description of the solvent based on the method of integral equations.[236–239] Detailed discussion of the application of these approaches has been reported;[237, 240] we will give only a brief outline of the calculation scheme. The interaction of the electron with molecules of the liquid results in redistribution of the solvent molecules, which is found from the electron–atom correlation functions $h_{es}(\boldsymbol{r})$ by solving integral equations [241]

$$\rho h_{es}(R) = \sum_j \int\int \omega_e(r) c_{ej}(|\boldsymbol{r} - \boldsymbol{r}'|)\chi_{sj}(|\boldsymbol{r}' - \boldsymbol{R}|)\mathrm{d}\boldsymbol{r}\mathrm{d}\boldsymbol{r}' , \qquad (43)$$

where $\omega_e(\boldsymbol{r})$ is the electronic CF, which is a quantum analogue of the IMCF; $c_{ej}(\boldsymbol{r})$ is the direct electron–atom CF, $\chi_{sj}(\boldsymbol{r})$ is the generalised susceptibility of the pure solvent. The electron correlation function $\omega_e(\boldsymbol{r})$ is related to the electron wave function as [237]

$$\omega_e(\boldsymbol{r}) \simeq \phi^2(\boldsymbol{r})$$

and can be calculated by the variation method [241, 242] or by solving the Schrödinger equation with the potential V_{ef}.[237] These studies of the hydrated electron (e_h) provide estimates for the energy and structural characteristics,[241, 242] which are in good agreement with experimental data: the calculated chemical potential e_h (see Ref. 241) differs from the experimental one [243] by only 1%.

Yet another interesting example of the solvation of quantum particles is study of the bipolaron — two excess electrons that form a bound state — a 'quasi-molecule'. Apparently, Feng *et al.* [244] were the first to investigate this problem in detail for a number of liquids on the basis of the continuum approach. The numerical investigations by the MC method for water [245] and for metal–ammonia solutions [235] have shown that the bipolaron states are stable in water and in metal–ammonia solutions at a metal concentration of $< 1\%$. As the concentration increases, the

Table 5. Kinetic (E_k), potential (E_p) and total (E_t) energies, chemical potential (μ) and average radius (r_e) of the hydrated electron and bipolaron calculated by various methods.

Method	E_k /eV	E_p /eV	E_t /eV	μ /eV	r_e /Å	Ref.
Electron						
QMD	2.2	−5.0	−2.8	−2.2	2.1	227
QMD	1.8	−3.6	−1.8	–	2.4	236
MSA	1.33	−5.57	−4.24	−1.13	2.5	238
MSA	1.8	−3.6	−1.8	–	2.2	236
RISM	1.84	−6.08	−4.26	−0.96	2.9	242
Bipolaron						
QMD $(H_2O)_{256}$	4.05	−16.4	−7.71	−1.57	2.6	245
MSA	2.34	−10.62	−9.67	−2.27	2.7	238

triplet state of the bipolaron decays, which is observed experimentally as a sharp decrease in the magnetic susceptibility.[246] On further increase in the metal concentration, bipolarons are clustered and the electrons become delocalised.[235, 247]

Both solvated electrons and bipolarons were studied using a hybrid approach which included the calculation of the electron structure by the density functional method and the solvent structure by the method of integral equations.[238] Table 5 presents the main energy parameters of the hydrated electron and bipolaron calculated by various methods, while Fig. 11 presents the electron–solvent correlation functions $g(r, \theta = 0)$ for a singlet bipolaron and an electron solvated in a model polar liquid consisting of hard spheres. Qualitative analysis has shown[248] that in the general case, the free energy functional includes various factors. The entropy contribution involved in the excluded volume cavity around the solute decreases the average radius of the bipolaron and favours an increase in its bond energy. The contribution caused by dielectric shielding produces an opposite effect. The competition of two contributions determines the stability condition for the bipolaron. The electron–electron correlations also result in an increase in the entropy factor due to the effects related to the formation of an 'exchange-correlation hole' and finally promote an increase in the bond energy. The calculations showed that bipolaron singlet states are stable in most polar liquids under normal conditions (Fig. 12).

The simplest example of a solvated quantum particle is positronium (Ps). This neutral quasi-atom consists of an electron and a positron. Like atomic hydrogen, positronium has two spin states separated in energy, namely, a singlet state (parapositronium) and a triplet state (orthopositronium). The interest in the study of this quasi-particle is related to the fact that, due to its electroneutrality, this particle can serve as a 'probe' for determining the character of molecular surfaces, the orientation of molecules in the liquid, and so on. Most often, continuum models are employed in the calculations of positronium. For example, a model taking into account the molecular structure of only the first coordination sphere of Ps has been considered.[249, 250] Monte Carlo calculations for positronium solutions[251] and for distribution of the Ps density in water have also been carried out.[252] A hybrid scheme for the calculation of hydrated positronium including self-consistent DFT computations of the distribution of the Ps density and the calculation of water microstructure by the method of integral equations has been developed.[253] The obtained results are consistent with experimental data. Figure 13 shows the Ps–H and Ps–O atom–atom correlation functions calculated for normal conditions. The form of these functions is typical of neutral solutes; however, in the case of positronium, they are smoother than in the case of neutral atoms. The procedure similar to that described in the study cited[253] is fairly versatile and can be used for solving a broad range of problems related to the study of solvated positronium.

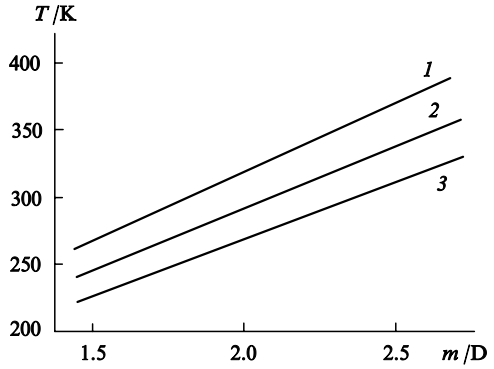


Figure 12. Diagram of bipolaron decomposition into single solvated electrons.[238]
Bipolarons are stable in the regions below the lines and decompose with temperature rise.
$\rho_0\sigma^3$: 0.8 (*1*), 0.9 (*2*), 1.0 (*3*).

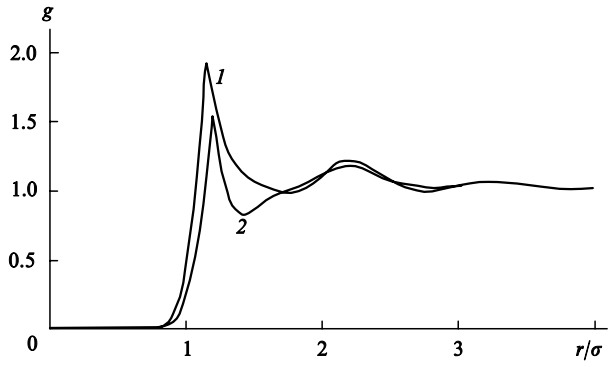


Figure 11. Electron–solvent correlation function $g(r, \theta = 0)$ in the spherical coordinates for an electron (*1*) and a singlet bipolaron (*2*) solvated in a polar liquid as solid spheres with the radius $\sigma = 3.15$ Å and the dipole moment $m = 1.6$ D with the value $\rho\sigma^3 = 0.9$ (ρ is the average density of the solvent) at $T = 233$ K.[238]

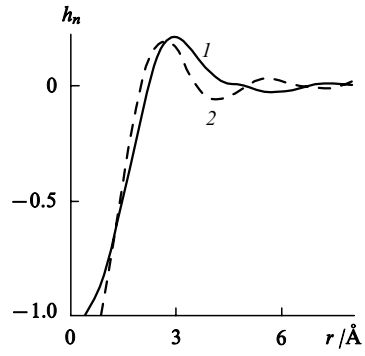


Figure 13. Correlation functions Ps–H (*1*) and Ps–O (*2*) for the positronium hydrated at room temperature.[253]

X. Tautomeric and conformational equilibria

The main goal of most molecular models of solvation is to study the conformational, tautomeric and other transformations of the solutes and to elucidate the conditions of formation of their dimers or other complexes. The scope of application of molecular models is very broad; therefore, without going into details, we

would only note characteristic features of the computation protocols involved.

Examples of application of the molecular models of solvation were given in the review.[40] This list is not exhaustive but continuum approaches clearly predominate. They are included in most packages of quantum-chemical programs and are most important in the study of binding of various ligands to the solute and in the studies related to the problem of 'recognition' in biomacromolecular reactions.[254, 255]

In the case of continuum methods, several preferable schemes can be distinguished. Comparison of the calculations of the conformations of various peptides has shown [256] that the GBSA model and the continuum calculations based on the solution of the Poisson – Boltzmann equation are best suited for the modelling of conformations. The corresponding estimates of the energy of conformational transitions give an error not exceeding 1 – 2 kcal mol^{-1} (see Ref. 256). The continuum models with distance-dependent $\varepsilon(r)$ are less suitable for these purposes. The accuracy of calculations in terms of the GBSA model depends appreciably on the approximation of the cavity.[40] The calculations in which the whole region occupied by the solute is approximated as a single spherical or ellipsoidal cavity produce unrealistic results.

At present, various hybrid methods are used in which the electronic structure of the solute is calculated without taking into account the medium, then charge distribution on the solute is determined and, finally, the local structure of the solvent for the resulting charge distribution is calculated in terms of the MD or MC procedures.[257] Unlike the continuum approaches, these calculations allow, in principle, not only estimation of the energy of conformational transitions and stability of the conformers but also determination of the enthalpy and entropy contributions to ΔG and the temperature dependence of the conformational transitions. They also provide the possibility of determining the accuracy of the classical molecular models. Comparison of the calculations using classical and hybrid models has shown, in particular, that the former give unsatisfactory results in the study of solvation of transition metal ions and polarisation of the solute molecule, while the latter produce more realistic results.[258]

In recent years, studies have been reported (see, for example, Refs 212 – 214) in which solvation was calculated in terms of a hybrid self-consistent procedure where the electronic structure of a conformer or a tautomer was calculated by quantum-chemical methods and the solvent microstructure was calculated by solving integral equations. These RISM – SCF models allow one to study chemical reactions in molecular liquids. The calculations were carried out for solute isomerisation in water [213, 220] and tautomerisation in acetylacetone.[219] The absolute values of the solvation parameters determined on the basis of integral equations do not always correspond to experimental data; however, such estimates are rather efficient for predicting thermodynamic and structural characteristics of the solvated complexes in various reactions (Table 6). In general, they are markedly more accurate than continuum models and almost as accurate as hybrid methods.

Table 6. Thermodynamic characteristics (kcal mol^{-1}) of some reactions for solute molecules.

Reaction	Solvent	ΔG	ΔH	$T\Delta\Gamma$	Ref.
Tautomerisation of	H_2O	−1.37 (−0.98)	−6.05 (2.7 ± 0.3)	−4.6 (3.7)	219
acetylacetone	DMSO	0.14 (0.29)	0.55 (1.8 ± 0.2)	0.41 (1.5)	219
	CCl_4	0.11 (1.74)	1.02 (2.5 ± 0.3)	0.91 (0.8)	219
pyridine	H_2O	−3.9 (−4.6 ± 0.8)	–	–	159
Anomerisation	H_2O	−3.23	−4.20	−0.96	213

Note. The values in parentheses are experimental results.

XI. Electronic spectra and solvatochromic shifts

The most detailed simulation of electronic spectra was carried out for the solvated electron. The absorption spectra of the solvated electron in ammonia,[224] methanol,[259] water [225] and heavy water [232] were calculated. The resulting dependences of the absorption maximum and the peak width on the temperature and solvent density are in quantitative agreement with experimental results. The isotope effects [232] and the dynamics of variation of the spectrum [260] have been studied in terms of nonadiabatic [259] and adiabatic [224] MD calculations. Simulation of the spectra of the solvated electron by the method of integral equations has been reported. These calculations also reproduce adequately the influence of temperature and ion concentration on the pattern of the absorption spectrum.[261] Figure 14 shows the calculated and experimental values for the shift of the absorption maximum of the hydrated electron in aqueous solutions of LiCl, $MgCl_2$ and $LiClO_4$.

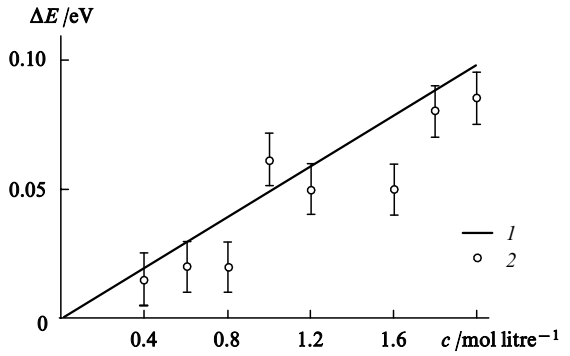


Figure 14. Shift of the maximum in the absorption spectrum of the hydrated electron in water – salt solutions depending on the salt concentration;
(*1*) calculation,[261] (*2*) experiment.[262]

Study of the solvatochromic shifts occupies an important place, especially in organic chemistry. There exists a correlation between the solvatochromic shift and the rates of chemical reactions in polar solvents.[1, 263] The possibility of constructing polarity scales and using chromophores as probes for determining the relative polarity of the solvent has long been discussed.[1] The data obtained in this way provide much more detailed knowledge of the intermolecular potentials than conventional dielectric measurements, as solvatochromic shifts are sensitive to both electrostatic and short-range interactions.

We will briefly discuss some features of calculation of these shifts using betaine-30 as an example. The simplest approach used is based on the mean-spherical approximation,[264] according to which the solvatochromic shift (v_s) and the free energy of solvation (ΔG) are related as follows

$$v_s = \Delta G \frac{m_e(m_g - m_e)}{a^3}, \qquad (44)$$

where m_e and m_g are the dipole moments of the solute in the ground and excited states, respectively. The free energy of solvation depends, in turn, on the size of the solute a and the dielectric constant of the liquid

$$\Delta G = f(\varepsilon, a),$$

the calculation of the function $f(\varepsilon, a)$ according to the MSA method presents no difficulty.[265] Using this approximation and relation (44), the solvatochromic shifts of betaine-30 in 110 solvents were found;[264] the average deviation of the calculated values from experimental ones did not exceed 10%. It should be emphasised that two important points were taken into account, namely, the change in the dipole moment of the solute upon optical excitation and the predominant role of electrostatic interactions between the solute and the solvent.

It was shown using simple estimates [266] that the contributions of the dispersion and induction interactions are also significant for the calculation of solvatochromic shifts. However, the results of calculation for betaine-30 [267] where these interactions were taken into account indicate that electrostatic interactions play crucial role in the appearance of this shift, which is mainly determined by the change in the dipole moment of the solute. The simplest approximation that assumes proportionality between the solvatochromic shift and the dipole moment [267] leads to satisfactory results consistent with experimental data, although it is less accurate than hybrid calculations (Table 7). Shoeib *et al.*[172] have attempted to include additionally the contribution of the electron polarisation of the solute by means of an appropriate renormalisation of the free energy of solvation. However, comparison of the data obtained by Chong and Hirata [163] with the results of hybrid calculations [267] has shown that for this method, the role of electron polarisation is overestimated. According to calculations,[267] the contribution of the electron polarisation to the solvatochromic shift does not exceed 5%.

Table 7. Solvatochromic shift (cm^{-1}) for betaine-30 in various solvents according to experimental data [268] and calculations by various methods.[172, 267]

Solvent	Experiment	Calculation by		Calculation by Eqn (44)
		INDO [a]	RISM	
Carbon tetrachloride	–	410	31	170
Chloroform	–	920	570	850
Acetone	1490	2730	–	1170
Acetonitrile	1160	4260	790	1510
Ethanol	2170	3070	–	2110
Methanol	2140	3570	2930	2510

[a] Semiempirical quantum-chemical calculation.

In some publications, the solvatochromic shifts have been studied in terms of hybrid models.[269–271] Detailed self-consistent calculations [271] demonstrated that accounting of the solvent can be restricted to the first coordination sphere of the solute (Fig. 15).

Finally, we will consider the dynamics of Stokes shifts. Continuum models are successfully used to study the dynamics of solvation phenomena; the complex dielectric constant $\varepsilon(\omega)$ is used in these cases as a dynamic characteristic. Simple models [272–274] have used the Debye parametrisation

$$\varepsilon(\omega) = \varepsilon_\infty + \frac{\varepsilon_0 - \varepsilon_\infty}{1 - i\tau_D\omega},$$

where ε_0 and ε_∞ are the static and optical dielectric constants of the solvent, τ_D is the Debye relaxation time for the spherical approximation of the shape of the solute. There are different ways of modernisation of the Born model: more complex multimode parametrisation of the dielectric function, allowance made for the non-spherical shape of the solute molecule, account taken of the non-local electrostatic effects (as noted above, the last-mentioned point allows one to include the molecular structure of the solvent in the calculation scheme). The influence of the solute shape on the dynamics of Stokes shifts was first studied for the ellipsoidal cavities around the solute molecule [275, 276] and then for cavities

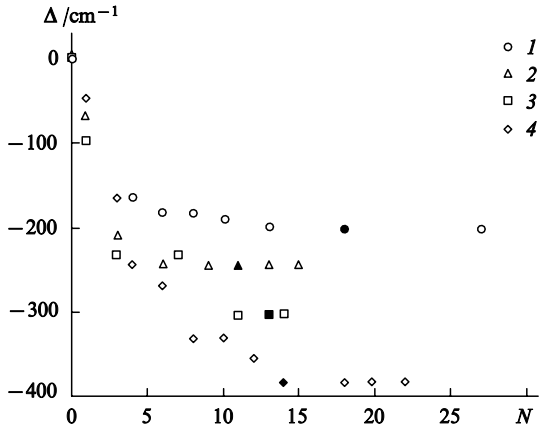


Figure 15. Calculated solvatochromic shift (Δ) *vs.* the number of solvent molecules (N) included in the quantum-chemical calculation.[271] (*1*) H_2O, (*2*) cyclo-C_6H_{12}, (*3*) C_6H_6, (*4*) CCl_4; the dark dots show the data for the first coordination sphere of the solute.

having an arbitrary shape.[277, 278] The molecular structure of the solvent was studied within the framework of the MSA method [279–281] and by other methods,[282, 283] and also using non-local models.[284] However, in all of these calculations, the solute was assumed to be spherical. Early studies were mainly concerned with the asymptotic behaviour of the temporal correlation functions and the possibility of determining these functions from experimental data using the Stokes shift.[272, 273, 276, 282, 283] The calculation could be improved if the data on the behaviour of the dielectric function in the region of medium and high frequencies, especially in the far infrared range, were available.[275, 278, 285] An upgraded continuum model has been used to perform a systematic study [286] of the influence of various factors on the dynamics of the Stokes shifts. In particular, the influence of the solute shape was studied in terms of single- and two-sphere models of the cavity surrounding the solute;[177] the intermediate spherical layer simulated the first coordination sphere of the solute. Yet another factor affecting the Stokes shift is related to the non-local effect.[31, 33] The simpler models of the cavity predict simple monoexponential kinetics of the shift for Debye solvents where a single relaxation mode of the medium is considered.[273, 274] This drawback is eliminated by taking into account either non-sphericity of the cavity [275, 276–278] or the multimode relaxation of the medium. In the latter case, the kinetics [286] is polyexponential and the results of calculations based on the local approach depend only slightly on the shape of the cavity. These calculations adequately reproduce the experimental data in the case where detailed information on the change in the dielectric constant is used as the input information.[275, 278, 286]

A more complex situation arises when the MSA model and the non-local theories are used. Even for Debye solvents and spherical solutes, the calculations lead to polyexponential kinetics.[279–281, 286] The local and non-local models produce different results. In non-local models, the oscillations of the correlation functions in the 0.1 ps $< t <$ 1 ns range are smoother than in local approaches. These oscillations, which are not typical of the changes in the Stokes shifts observed experimentally, arise in all local models irrespective of the approximation of the solute shape. Another important difference is related to the asymptotic behaviour of the correlation functions. Non-local models yield much longer relaxation times than local models.[286]

XII. Electron transfer

Electron transfer plays a key role in many chemical and biological processes,[287] and study of the electron transfer occupies an important place among applications of the molecular models of

solvation. The most important characteristic of this process is the rate constant for transfer K_{et} . In the Frank – Condon approximation in which the matrix element of the electron transition V_{et} does not depend on the nuclear coordinates, the constant can be found from the following equation:[287–289]

$$K_{et} = V_{et}^2 \sqrt{\frac{\pi\beta}{E_r}} \exp\left[-\frac{\beta(\Delta F^\circ + E_r)^2}{4E_r}\right], \quad (45)$$

where E_r is the reorganisation energy, ΔF° is the free energy of the reaction. The reorganisation energy is composed of the inner-sphere (*i.e.*, related to the internal degrees of freedom of the solute) and the outer-sphere (*i.e.*, related to the rearrangement of the solvent structure) components. In the continuum approach for spherically symmetrical charge distributions on the donor and the acceptor, outer-sphere reorganisation energy is often found from the equation [287]

$$E_r = C\Delta q^2 \left(\frac{1}{2a_A} + \frac{1}{2a_D} - \frac{1}{R_{DA}}\right), \quad (46)$$

where C is the Pekar factor, Δq is the charge being transferred, a_D and a_A are the effective radii for the donor and the acceptor, and R_{DA} is the distance of transfer. There exist numerous procedures for extending expressions (45) and (46) that take into account the real shape of the solute, quantum effects, deviations from the Frank – Condon approximation, and so on.[290] In particular, for the intramolecular transfer of an electron, the influence of high-frequency quantum modes of the solute is commonly taken into account in an explicit form.[291–298] However, in this case, too, the reorganisation energy E_r and the matrix element V_{et} still remain the key characteristics of the electron transfer. The problem is to elucidate the dependence of these values on the molecular and thermodynamic parameters of the surrounding medium. Here we discuss only aspects of the electron transfer concerned with its simulation on the basis of microscopic models and upgraded continuum theories.

Some effects cannot, in principle, be taken into account within the bounds of the continuum electrostatic models of the medium. These include, for example, the temperature dependence of the reorganisation energy. It can be included in a standard continuum calculation only through the temperature dependence of the dielectric constant of the solvent. However, this type of modelling is inefficient: the reorganisation energy really decreases with temperature rise,[293] whereas the theoretical estimate based on the data on the dielectric constant predicts an increase in this energy. The error of calculation is due to neglect of the temperature dependence of the size of the cavity occupied by the solute. The size and the shape of the cavity are fixed in the continuum calculation and only transition to the molecular description of the solvent provides the possibility of reproducing the desired effect.

The continuum theory (in the local electrostatic variant) also cannot explain the presence of a noticeable outer-sphere reorganisation energy in non-polar solvents (benzene, dioxane, *etc.*), whose molecules are devoid of a permanent dipole moment. In these media, $\varepsilon_\infty = \varepsilon_0$ and the Pekar factor C is equal to zero, while the reorganisation energies found experimentally are equal to 0.1 – 0.2 eV.[293]

The simplest way of correcting the continuum calculations is to use the mean-spherical approximation for the solute model as hard spheres with an electric charge (on the solute) or a dipole moment (for solvent molecules). This approximation allows one not only to calculate the reorganisation energy but also to estimate correctly its temperature dependence (Table 8); however, its use is restricted by the assumption concerning the spherical shape of the solute inherent in the MSA theory. This version of the MSA model has also been used [296, 297] to study the reorganisation energy for the same solute (approximated by a sphere) in a series of solvents with different polarity including non-polar solvents.[296, 297] An alternative way of upgrading the continuum theory [298] is to detail

Table 8. Calculated and experimental temperature characteristics of the free energy of solvation (ΔG) and reorganisation energy (E_r) for (tetrahydro-4H-thiopyran-4-ylidene)propanedinitrile dissolved in acetonitrile.[293]

Model	a /Å	ΔG /eV	$\frac{T\partial E_r}{\partial T}$ /eV	$\frac{T\partial \Delta G}{\partial T}$ /eV
Continuum	4.52	4.64	0.03	0.10
MSA	4.50	4.39	−0.19	0.37
Experiment	–	–	−0.23	0.32

the dielectric model of the medium. The solute is assumed to be surrounded by two cavities with different dielectric constants, namely, high-frequency and static ones (see Fig. 7). The cavities are constructed in the same way as in the PCM method. The modernised model explicitly takes into account the electronic structure and the real shape of the solute and implicitly, the molecular structure of the solvent in terms of the parameters of the cavity, *i.e.*, the dielectric constants and the atom radii r_∞ and r_{in}

$$r_\infty = k r_{VdW}, \quad (47)$$
$$r_{in} = \delta + r_\infty,$$

where k is a universal scale factor, r_{VdW} is the van der Waals radius, and δ depends on the particular solvent. This model can be used to calculate the reorganisation energy and the matrix element of transfer if these values depend little on the details of molecular structure around the solute. The optimal k and δ values are found by comparing the theoretical and experimental values for the free energy of solvation of small polyatomic ions.[298] The k and δ values obtained in this way were used to calculate the reorganisation energies for many reactions of intramolecular electron transfer in steroid compounds.[299] The results of calculations are consistent with experimental data,[291] which cannot be reproduced in the single-cavity model.[300–302] However, like other continuum theories, this method cannot describe the temperature dependence of the reorganisation energy.

The method of integral equations also allows one to take into account, in an explicit form, the discrete pattern of charge distribution on the solvent molecules. The reorganisation energy E_r was calculated, in terms of the RISM theory,[172] for betaine-30 solvated in various polar liquids. The results of calculations [172] are in qualitative agreement with experimental data. Yet another line in the research into electron transfer related to the effect of the molecular structure of the solvent on the reorganisation energy is represented by studies performed by MD calculations.[303–306] These works dealt with calculations of the diabatic surfaces of free energy, whose intersection area determines the transfer rate. In the macroscopic Marcus theory,[307] the potential surfaces of the reactants and products are parabolic. The MD calculations [305] have shown that the free energy surfaces found are close to parabolic surfaces, but under certain conditions, the reaction system behaviour can markedly deviate from the predictions of the Marcus theory [see Eqns (45) and (46)]. The deviations are great in the case of polarisation of neutral solutes,[308–310] *i.e.*, in charge separation processes. They have also been observed for charged asymmetrical systems with different structures of the donor and acceptor centres.[311] The deviations are assumed to be due to two compensative factors, namely, electrostriction and dielectric saturation, both being dependent on the charge of the reactants.[312] The MD calculations of the reorganisation energy have now been carried out for several simplified model systems of electron transfer [311–316] and for complex systems that mimic the electron transfer in proteins.[317, 318] Compared with routine MD calculations, these calculations require accurate handling of Coulomb interactions (see Section V) and taking into account electron polarisation. The latter is usually simulated by renorm-

alisation of the reorganisation energy by changing the Pekar factor C.[317]

The calculation of the matrix element V_{et} requires thorough quantum-chemical calculations.[292, 319] The result is sensitive to the choice of the initial and final diabatic electronic states between which the transition takes place. It is recommended to localise these states by the generalised Mulliken – Hush method according to which they are determined by diagonalisation of the matrix of the dipole moment of the electron transition.[290, 320] An alternative method invariant with respect to the choice of the basis states has also been formulated.[299] For complex biochemical objects, direct quantum-chemical calculation of the matrix elements V_{et} is impossible; therefore, it was proposed to estimate this matrix element by calculating the quasi-classical tunnelling flow of probability.[321 – 324]

The number of works dealing with the effect of the solvent on the matrix element V_{et} is relatively low (see the review [292]). These calculations are based on upgraded continuum models [299] or molecular schemes,[317] which allow one to determine the contribution of the effect of the molecular structure of the solute (conformation and effective radius) on the V_{et} value. This is exemplified in Table 9, which presents the results of calculation of characteristics of the electron transfer for a number of model $(CH_2)_n^-$ anions. The results confirm the tendency of V_{et} for exponential decrease following an increase in the distance R_{DA} between the donor and the acceptor, which has been discussed in the literature.[290]

Table 9. Calculated characteristics of electron transfer for a number of model $(CH_2)_n^-$ anions with the linear structure.[299]

n	E_r /eV	ΔF /eV	$10^3\ V_{et}$ /eV	R_{DA} /Å
4	0.86	0.035	257.0	3.80
6	1.37	0.28	61.9	6.26
8	1.70	0.41	14.7	8.74
10	1.92	0.48	3.77	11.23

XIII. Conclusion

The examples considered above of the use of molecular models for the study of solvation in polar liquids permit one to estimate qualitatively and, in some cases, even quantitatively the influence of the solvent on the change in the structural and thermodynamic properties of solvated particles and to study the physicochemical processes that accompany solvation. In essence, the molecular approach is meant to take into account two factors. The first one is mainly of entropic origin and is related to the excluded volume effect and the packing of molecules in the nearest environment of the solute particles. It is a consequence of the finite size of these particles. The second factor is due to the finite size of the solvent particles that interact with the solute. Both factors were ignored in the early solvation theories. In the modern continuum theories, the former factor is consistently taken into account, in particular, the size and shape of the solute are considered explicitly by specifying an excluded volume cavity in the continuum medium. This description is valid in the asymptotic limit

$$\frac{\text{size of the solvent particles}}{\text{size of the solute particles}} \ll 1$$

The theories that are commonly called molecular are beyond the scope of this restriction.

In the simplest molecular models of solvation, the solute and solvent particles are considered to be spherical, with point charges or dipoles at the centre of the sphere. At this level of description, it is usually possible to obtain analytical expressions or semianalytic algorithms for the calculation of the response field, the solvation energy and other values. Abandoning of the spherical approximation, which is absolutely necessary for calculating real systems, inevitably converts the model physical theory into a cumbersome computation procedure. The computations are least cumbersome in the continuum approximation, whereas the use of 'truly' molecular calculations (MC or MD) increases the computational burden by a factor of 10^3 or more. The calculations of the correlation functions by the method of integral equations occupy an intermediate position, as regards laboriousness, in the series of modern computational methods of the solvation theory.

It is noteworthy that the structure of the medium can be ignored if the difference between the solute and solvent particles is much greater than the size of solvent particles. In this case, one can use hybrid schemes, which smoothly 'sew together' the continuum and molecular modes of the description of solvation effects and thus reduce the computational burden without substantial decrease in the reliability of the results obtained.

It is shown using particular examples that molecular models can be efficiently utilised to study various solvation systems ranging from salt solutions to dissolved biomacromolecules. The possibility of developing hybrid schemes in order to take into account changes in the conformation and the electronic structure of molecules in the solvent extends the scope of application of molecular models. The prospects of nanotechnology are associated with the study of a large number of complex liquids, which are characterised by high microheterogeneity and diverse supramolecular architecture which arises on the mesoscopic scale.[325] The molecular models can serve as peculiar probes in the study of these mesoscopic structures, and new interesting results may be expected in this field.

This work was supported by the Russian Foundation for Basic Research (Project Nos 01-03-53529, 01-04-97032, 02-03-33049, 00-15-97295 and 01-03-07013) and by the RFBR – INTAS (Grant No. 97-03-71049).

References

1. C Reichardt *Solvents and Solvent Effect in Organic Chemistry* (Weinheim: VCH, 1988)
2. A A Vedenov *Fizika Rastvorov* (Physics of Solutions) (Moscow: Nauka, 1984)
3. R R Dogonadze, A A Kornyshev, J Ulstrup, in *The Chemical Physics of Solvation* (Amsterdam: Elsevier, 1985) p. 3
4. M Born *Z. Phys.* **1** 45 (1920)
5. A N Lagar'kov, V M Sergeev *Usp. Fiz. Nauk* **125** 409 (1978) [a]
6. B Ya Simkin, I I Sheikhet *Kvantovo-Khimicheskaya i Statisticheskaya Teoriya Rastvorov* (Quantum-Chemical and Statistical Theory of Solutions) (Moscow: Khimiya, 1989)
7. D W Heerman *Computer Simulation Methods in Theoretic Physics* (Berlin: Springer, 1986)
8. *Metod Molekulyarnoi Dinamiki v Fizicheskoi Khimii* (Method of Molecular Dynamics in Physical Chemistry) (Moscow: Nauka, 1996)
9. V N Zamalin, E G Norman, V S Filinov *Metody Monte-Karlo v Statisticheskoi Termodinamike* (Monte Carlo Methods in Statistical Thermodynamics) (Moscow: Nauka, 1977)
10. K Binder *Monte Carlo Methods in Statistical Physics* (Berlin: Springer, 1979)
11. G A Kaminski, W L Jorgensen *J. Phys. Chem. B* **102** 1787 (1998)
12. R M Lynden-Bell, J C Rasaiah *J. Chem. Phys.* **107** 1981 (1997)
13. R M Levy, E Gallicchio *Annu. Rev. Phys. Chem.* **49** 531 (1998)
14. D Frenkel, B Smit *Understanding Molecular Simulation* (San Diego: Academic Press, 1996)
15. P G Mortimer, in *Physical Chemistry* (San Diego: Harcourt Academic Press, 1993) p. 200
16. M P Allen, D J Tildesley *Computer Simulation of Liquids* (Oxford: Clarendon, 2000)
17. A J Stone *The Theory of Intermolecular Forces* (Oxford: Clarendon, 1996)

18. S Weiner, P Kollman, D Case, U Singh, C Ghio, G Alagona, S Profeta Jr, P Weiner *J. Am. Chem. Soc.* **106** 765 (1984)
19. B R Brooks, R E Bruccoleri, B D Olafson, D J States, S Swaminathan, M Karplus *J. Comput. Chem.* **4** 187 (1983)
20. W L Jorgensen, T B Nguyen *J. Comput. Chem.* **14** 195 (1993)
21. W F Van Gunsteren, S R Billeter, A A Eising, P H Hunenberger, P Kruger, A E Mark, W R P Scott, I G Tironi *Biomolecular Simulation: the GROMOS'96 Manual and User Guide* (Zurich, Groningen: Hochschulverlag AG, 1996)
22. D van der Spoel, P J Maaren, H J C Berendsen *J. Chem. Phys.* **108** 10220 (1998)
23. C G Gray, K E Gubbins *Theory of Molecular Liquids* (Oxford: Oxford University Press, 1984)
24. A A Kornyshev, M A Vorotyntsev *Elektrostatika Sred s Prostranstvennoi Dispersiei* (Electrostatics of Media with Spatial Dispersion) (Moscow: Nauka, 1993)
25. T Clark *A Handbook of Computational Chemistry* (New York: Wiley, 1985)
26. V M Agranovich, V L Ginzburg *Spatial Dispersion in Crystal Optics and Theory of Exitons*. Interscience London 1966
27. A A Kornyshev, in *The Chemical Physics of Solvation* (Amsterdam: Elsevier, 1985) p. 77
28. R R Dogonadze, A A Kornyshev *Phys. Status Solidi B* **53** 439 (1972)
29. R R Dogonadze, A A Kornyshev *J. Chem. Soc., Faraday Trans. 2* **70** 1121 (1974)
30. M A Vorotyntsev *J. Phys. C* **11** 3323 (1978)
31. M Basilevsky, D Parsons *J. Chem. Phys.* **108** 9107 (1998)
32. A A Kornyshev, A I Rubinshtein, M A Vorotyntsev *J. Phys. C* **11** 3307 (1978)
33. M Basilevsky, D Parsons *J. Chem. Phys.* **105** 9734 (1996)
34. R Kubo, M Toda, N Hatshisuma *Statistical Physics* Vol. 2 (Berlin: Springer, 1985)
35. J Kirkwood *J. Chem. Phys.* **7** 39 (1939)
36. J Tomasi, M Persico *Chem. Rev.* **94** 2027 (1994)
37. J Tomasi, B Menucci, R Cammi, M Cossi In *Theoretical Aspects of Biochemical Reactivity* (Eds G Naray-Szabo, A Warshel) (Dordrecht: Kluwer, 1997) p. 1
38. J-L Rivail, D Rinaldi, Kluwer, in *Computational Chemistry, Review of Current Trends* (Ed. J Leszczynski) (New York: World Scientific, 1995) p. 139
39. C J Cramer, D G Truhlar, in *Reviews in Computational Chemistry* (Eds K B Lipkowitz, D B Boyd) (New York: VCH, 1995) p. 1
40. C J Cramer, D G Truhlar *Chem. Rev.* **99** 2161 (1999)
41. C J Cramer, D G Truhlar, in *Solvent Effects and Chemical Reactivity* (Eds O Tapia, J Bertran) (Dordrecht: Kluwer, 1996) p. 1
42. N G J Richards, in *Molecular Orbital Calculations for Biological Systems* (Ed. A-M Sapse) (New York: Oxford University Press, 1998) p. 11
43. A A Rashin, M A Bukatin *Biophys. Chem.* **51** 167 (1994)
44. J L Rivail *C. R. Acad. Sci. (Paris)* **311** 307 (1990)
45. F J Olivares del Valle, J Tomasi *Chem. Phys.* **150** 139 (1991)
46. M A Aguilar, F J Olivares del Valle, J Tomasi *Chem. Phys.* **150** 151 (1991)
47. M W Wong, K B Wiberg, M J Frisch *J. Am. Chem. Soc.* **114** 523 (1992)
48. A A Rashin, L Young, I A Topol *Biophys. Chem.* **51** 359 (1994)
49. R B Murphy, R A Friesner, M N Ringnalda, W A Goddard *J. Chem. Phys.* **101** 2986 (1994)
50. D J Tannor, B Marten, R B Murphy, R A Friesner, D Sitkoff, A Nicholls, M Ringnalda, W A Goddard *J. Am. Chem. Soc.* **116** 11 875 (1994)
51. A A Rashin, M A Bukatin, J Andzelm, A T Hagler *Biophys. Chem.* **51** 375 (1994)
52. G J Tawa, R L Martin, L R Pratt, T V Russo *J. Phys. Chem.* **100** 1515 (1996)
53. A Fortunelli, J Tomasi *Chem. Phys. Lett.* **231** 34 (1994)
54. S Cabani, P Gianni, V Mollica, L Lepori *J. Solution Chem.* **10** 563 (1981)
55. Y Ding, D N Bernardo, R M Levy *J. Phys. Chem.* **99** 11575 (1995)
56. M Bachs, F J Luque, M Orozco *J. Comput. Chem.* **15** 446 (1994)
57. C J Cramer, D G Truhlar *J. Comput. Aided Mol. Des.* **6** 629 (1992)
58. P-Y Morgantini, P A Kollman *J. Am. Chem. Soc.* **117** 6057 (1995)
59. B Marten, K Kim, C Cortis, R A Friesner, R B Murphy, M N Ringnalda, D Sitkoff, B Honig *J. Phys. Chem.* **100** 11775 (1996)
60. B Lee, F M Richards *J. Mol. Biol.* **55** 379 (1971)
61. W C Still, A Tempczyk, R C Hawley, T Hendrickson *J. Am. Chem. Soc.* **112** 6127 (1990)
62. D Qiu, P S Shenkin, F P Hollinger, W C Still *J. Phys. Chem. A* **101** 3005 (1997)
63. C J Cramer, D G Truhlar *J. Am. Chem. Soc.* **113** 8305 (1991)
64. C J Cramer, D G Truhlar *Science* **256** 213 (1992)
65. C Amovilli, B Mennucci *J. Phys. Chem. B* **101** 1051 (1997)
66. C Colominas, F J Luque, J Teixido, M Orozco *Chem. Phys.* **240** 253 (1999)
67. B Honig, K Sharp, A-S Yang *J. Phys. Chem.* **97** 1101 (1993)
68. V K Misra, K A Sharp, R A Friedman, B Honig *J. Mol. Biol.* **238** 245 (1994)
69. D Sitkoff, K A Sharp, B Honig *J. Phys. Chem.* **98** 1978 (1994)
70. D Rinaldi, J-L Rivail *Theor. Chim. Acta* **32** 57 (1973)
71. O Christiansen, K V Mikkelsen *J. Chem. Phys.* **110** 1365 (1999)
72. L Onsager *J. Am. Chem. Soc.* **58** 1486 (1936)
73. B Jaryaram, D Sprous, D L Beverdge *J. Phys. Chem.* **102** 9571 (1998)
74. X Zou, Y Sun, I D Kuntz *J. Am. Chem. Soc.* **121** 8033 (1999)
75. S Miertus, E Scrocco, J Tomasi *Chem. Phys.* **55** 117 (1981)
76. J Tomasi *J. Comput. Chem.* **16** 1449 (1995)
77. M Cossi, V Barone, R Cammi, J Tomasi *Chem. Phys. Lett.* **255** 327 (1996)
78. F J Luque, J M López, M Orozco *Theor. Chem. Acc.* **103** 343 (2000)
79. M V Basilevsky, G E Chudinov *Chem. Phys.* **157** 327 (1991)
80. J Tomasi, B Mennucci, E Cances *J. Mol. Struct.* **464** 211 (1999)
81. A Klamt, G Schürmann *J. Chem. Soc., Perkin Trans. 2* 799 (1993)
82. D M York, M Karplus *J. Phys. Chem. A* **103** 11060 (1999)
83. S W Rick, B J Berne *J. Am. Chem. Soc.* **116** 3949 (1994)
84. J Åqvist, T Hansson *Phys. Chem.* **100** 9512 (1996)
85. G Hummer, L R Pratt, A E Garcúa *J. Phys. Chem. A* **102** 7885 (1998)
86. P A Monson, G P Morris *Adv. Chem. Phys.* **77** 451 (1990)
87. I R Yukhnovskii, M F Golovko *Statisticheskaya Teoriya Klassicheskikh Ravnovesnykh Sistem* (Statistical Theory of Classical Equilibrium Systems) (Kiev: Naukova Dumka, 1980)
88. G A Martynov *Fundamental Theory of Liquids* (Bristol: Adam Hilger, 1992)
89. G N Sarkisov *Usp. Fiz. Nauk* **169** 625 (1999) [*Physics-Uspekhi* **42** 545 (1999)]
90. D Chandler, H C Andersen *J. Chem. Phys.* **57** 1930 (1972)
91. P T Cummings, G Stell *Mol. Phys.* **46** 383 (1982)
92. L Lue, D Blankstein *J. Chem. Phys.* **96** 8528 (1992)
93. D Chandler, R Silbey, B M Ladanyi *Mol. Phys.* **46** 1335 (1982)
94. L Lue, D Blankstein *J. Chem. Phys.* **102** 5427 (1995)
95. S J Singer, D Chandler *Mol. Phys.* **55** 621 (1985)
96. H-A Yu, B Roux, M Karplus *J. Chem. Phys.* **92** 5020 (1990)
97. M J Gillan *Mol. Phys.* **38** 1781 (1979)
98. S Labik, A Malijevsky, P Vonka *Mol. Phys.* **56** 709 (1985)
99. C Caccamo *Phys. Rep.* **274** 1 (1996)
100. E Waisman, J L Lebowitz *J. Chem. Phys.* **52** 4307 (1970)
101. L Blum *J. Chem. Phys.* **61** 2129 (1974)
102. M Ikeguchi, J Doi *J. Chem. Phys.* **103** 5011 (1995)
103. D Beglov, B Roux *J. Phys. Chem. B* **101** 7821 (1997)
104. Q Du, D Beglov, B Roux *J. Phys. Chem. B* **104** 796 (2000)
105. A Kovalenko, F Hirata *Chem. Phys. Lett.* **290** 237 (1998)
106. C M Cortis, P J Rossky, R A Friesner *J. Chem. Phys.* **107** 6400 (1997)
107. A Kovalenko, F Hirata *J. Chem. Phys.* **113** 2793 (2000)
108. A Kovalenko, T N Truong *J. Chem. Phys.* **113** 7458 (2000)
109. J Richardi, P H Fries, R Fischer, S Rast, H Krienke *J. Mol. Liq.* **73–74** 465 (1997)
110. J Richardi, C Millot, P H Fries *J. Chem. Phys.* **110** 1138 (1999)
111. J S Bader, D Chandler *J. Phys. Chem.* **96** 6423 (1992)
112. P H Hünenberger, W F van Gunsteren *J. Chem. Phys.* **108** 6117 (1998)
113. I G Toroni, R Sperb, P E Smith, W F van Gunsteren *J. Chem. Phys.* **102** 5451 (1995)

114. H Resat, J A McCammon *J. Chem. Phys.* **108** 9617 (1998)
115. P P Ewald *Ann. Phys. (Leipzig)* **64** 253 (1921)
116. G Hummer, D M Soumpasis, M Neumann *Mol. Phys.* **77** 769 (1992)
117. G Hummer, D M Soumpasis, M Neumann *J. Phys.: Condens. Matter.* **6** A141 (1994)
118. G Hummer, L R Pratt, A E Garcia *J. Chem. Phys.* **107** 9275 (1997)
119. G Hummer, L R Pratt, A E Garcia, M Neumann, in *Simulation and Theory of Electrostatic Interactions in Solution* (Eds L R Pratt, G Hummer) (New York: AIP Press, 1999)
120. F Figueirido, G S Del Buono, R M Levy *J. Chem. Phys.* **103** 6133 (1995)
121. F Figueirido, G S Del Buono, R M Levy *J. Phys. Chem. B* **101** 5622 (1997)
122. M V Vener, I V Leontyev, Yu A Dyakov, M V Basilevsky, M D Newton *J. Phys. Chem. B* **106** 13078 (2002)
123. A Ben-Naim, Y Marcus *J. Chem. Phys.* **81** 2016 (1984)
124. G Hummer, S Garde, A E Garcia, L R Pratt *Chem. Phys.* **258** 349 (2000)
125. H S Ashbaugh, T M Truskett, P G Debenedetti *J. Chem. Phys.* **116** 2907 (2002)
126. T R Rettich, Y P Handa, R Batino, E Wilhelm *J. Phys. Chem.* **85** 3230 (1980)
127. K Lum, D Chandler, J D Weeks *J. Phys. Chem. B* **103** 4570 (1999)
128. R A Pierotti *Chem. Rev.* **76** 717 (1976)
129. F H Stillinger *J. Solution Chem.* **2** 141 (1973)
130. H Reiss, H L Frisch, J L Lebowitz *J. Chem. Phys.* **31** 369 (1959)
131. H Reiss *Adv. Chem. Phys.* **9** 1 (1965)
132. M Irisa, K Nagayama, F Hirata *Chem. Phys. Lett.* **207** 430 (1993)
133. M Irisa, T Takahashi, K Nagayama, F Hirata *Mol. Phys.* **85** 1227 (1995)
134. E Gallicchio, M M Kubo, R M Levy *J. Phys. Chem. B* **104** 6271 (2000)
135. J Wang, W Wang, S Huo, M Lee, P A Kollman *J. Phys. Chem. B* **105** 5055 (2001)
136. L R Pratt, D Chandler *J. Chem. Phys.* **67** 3683 (1977)
137. L R Pratt *Chem. Rev.* **102** 2671 (2002)
138. A Pohorille, L R Pratt *J. Am. Chem. Soc.* **112** 5066 (1990)
139. D Beveridge, F Di Capua *Annu. Rev. Biophys. Chem.* **18** 431 (1989)
140. W Jorgensen *Acc. Chem. Res.* **22** 184 (1989)
141. P Kollman *Chem. Rev.* **93** 2395 (1993)
142. T C Beutler, W F van Gunsteren *J. Chem. Phys.* **101** 1417 (1994)
143. B Guillot, Y Guissani, S Bratos *J. Chem. Phys.* **95** 3643 (1991)
144. B Guillot, Y Guissani *J. Chem. Phys.* **99** 8075 (1993)
145. L R Pratt, A Pohorille *Proc. Natl. Acad. Sci. USA* **89** 2995 (1992)
146. T C Beutler, D R Beguelin, W F van Gunsteren *J. Chem. Phys.* **102** 3787 (1995)
147. F M Floris, M Selmi, A Tani, J Tomasi *J. Chem. Phys.* **107** 6353 (1997)
148. J Tomas-Oliveira, S J Wodak *J. Chem. Phys.* **111** 8576 (1999)
149. G Hummer, S Garde, A E Garcia, A Pohorille, L R Pratt *Proc. Natl. Acad. Sci. USA* **93** 8951 (1996)
150. S Garde, A E Garcia, L R Pratt , G Hummer *Biophys. Chem.* **78** 21 (1999)
151. G Hummer, S Garde, A E Garcia, M E Paulaitis, L R Pratt *J. Phys. Chem. B* **102** 10469 (1998)
152. G Hummer, S Garde *Phys. Rev. Lett.* **80** 4193 (1998)
153. X Kong, C L Brooks *J. Chem. Phys.* **105** 2414 (1996)
154. R Pomgs, E Eisenmesser, C B Post, B Roux *J. Chem. Phys.* **111** 3387 (1999)
155. H S Ashbaugh, M E Paulaitis *J. Phys. Chem.* **100** 1900 (1996)
156. S R Durell, A Wallqvist *Biophys. J.* **71** 1695 (1996)
157. N Matubayasi, L H Reed, R M Levy *J. Phys. Chem.* **98** 10640 (1994)
158. S H Fleischman, C L Brooks *J. Chem. Phys.* **87** 3029 (1987)
159. L Shao, H-A Yu, J Gao *J. Phys. Chem. A* **102** 10366 (1998)
160. C C Chambers, G D Hawkins, C J Cramer, D G Truhlar *J. Phys. Chem.* **100** 16385 (1996)
161. G Hummer *J. Am. Chem. Soc.* **121** 6299 (1999)
162. G Hummer, L R Pratt, A E Garcia *J. Phys. Chem.* **100** 1206 (1996)
163. C-H Chong, F Hirata *J. Phys. Chem. B* **101** 3209 (1997)
164. O Ya Samoilov *Discuss. Faraday Soc.* **24** 133 (1957)
165. J Florian, A Warshel *J. Phys. Chem. B* **101** 5583 (1997)
166. Y Marcus *J. Chem. Soc., Faraday Trans. 1* **82** 233 (1986)
167. H Friedman, C V Krishnan, in *Water: A Comprehensive Treatise* (Ed. F Franks) (New York: Plenum, 1973)
168. T Kerdcharoen, B M Rode *J. Phys. Chem. A* **104** 7073 (2000)
169. D Marx, M E Tuckerman, M Parrinello *J. Phys.: Condens. Matter.* **12** A153 (2000)
170. H-A Yu, B Roux, M Karplus *J. Phys. Chem.* **94** 4683 (1990)
171. G D Hawkins, C J Cramer, D G Truhlar *J. Phys. Chem.* **100** 19824 (1996)
172. T Shoeib, G D Ruggiero, K W M Sin, A C Hopkinson, I H Williams *J. Chem. Phys.* **117** 2762 (2002)
173. P L Cummins, J E Gready *J. Comput. Chem.* **20** 1028 (1999)
174. V Barone, M Cossi, J Tomasi *J. Comput. Chem.* **19** 404 (1998)
175. D L Beveridge, G W Schnuelle *J. Phys. Chem.* **79** 2562 (1975)
176. M H Abraham, J Liszi, L Meszaros *J. Chem. Phys.* **70** 2491 (1979)
177. M Basilevsky, I Rostov, M Newton *Chem. Phys.* **232** 189 (1998)
178. D Y C Chan, D J Mitchell, B Ninham *J. Chem. Phys.* **70** 2946 (1979)
179. S Wertheim *J. Chem. Phys.* **55** 4291 (1971)
180. W R Fawcett, L Blum *Chem. Phys. Lett.* **187** 173 (1991)
181. A A Rashin, B Honig *J. Phys. Chem.* **89** 5588 (1985)
182. J-K Hyun, T Ichiye *J. Phys. Chem. B* **101** 3596 (1997)
183. J-K Hyun, T Ichiye *J. Chem. Phys.* **109** 1074 (1998)
184. P H Fries, W Kunz, P Calmettes, P Turq *J. Chem. Phys.* **101** 554 (1994)
185. F Hirata, P J Rossky *Chem. Phys. Lett.* **83** 329 (1983)
186. J S Perkyns, B M Pettitt *Chem. Phys. Lett.* **190** 626 (1992)
187. M Kinoshita, F Hirata *J. Chem. Phys.* **106** 5202 (1997)
188. J Richardi, P H Fries, H Krienke *J. Chem. Phys.* **108** 4079 (1998)
189. A Kovalenko, F Hirata *J. Chem. Phys.* **112** 10403 (2000)
190. S W Rick, in *Simulation and Theory of Electrostatic Interactions in Solution* (Eds L R Pratt, G Hummer) (New York: AIP Press, 1999)
191. Y P Liu, K Kim, B J Berne, R A Friesner, S W Rick *J. Chem. Phys.* **108** 4739 (1998)
192. H A Stern, G A Kaminski, J L Banks, R Zhou, B J Berne, R A Friesner *J. Phys. Chem. B* **103** 4730 (1999)
193. H A Stern, F Rittner, B J Berne, R A Friesner, S W Rick *J. Chem. Phys.* **115** 2237 (2001)
194. S W Rick, S J Stuart, B J Berne *J. Chem. Phys.* **101** 6141 (1994)
195. M W Mahoney, W L Jorgensen *J. Chem. Phys.* **112** 8910 (2000)
196. H Saint-Martin, J Hernandez-Cobos, M I Bernal-Uruchurtu, I Ortega-Blanke, H J C Berendsen *J. Chem. Phys.* **113** 10 899 (2000)
197. G J Kell *J. Chem. Eng. Data* **20** 97 (1975)
198. K Krynicki, C D Green, D W Sawyer *Faraday Discuss. Chem. Soc.* **66** 199 (1978)
199. J Jonas, T De Fries, D J Wilbur *J. Chem. Phys.* **65** 582 (1976)
200. D Bertolini, M Cassettari, G Salvetti *J. Chem. Phys.* **76** 3285 (1982)
201. A D Buckingham *Proc. R. Soc. London, Ser. A* **238** 235 (1956)
202. P Amara, M J Field, C Alhambra, J Gao *Theor. Chem. Acc.* **104** 336 (2000)
203. S R Kimura, R C Brower, C Zhang, M Sugimori *J. Chem. Phys.* **112** 7723 (2000)
204. R H Wood, E M Yezdimer, S Sakane, J A Barriocanal, D J Doren *J. Chem. Phys.* **110** 1329 (1999)
205. D A Tikhonov, R V Polozov, E G Timoshenko, Yu A Kuznetsov, A V Gorelov, K A Dawson *J. Chem. Phys.* **109** 1528 (1998)
206. A Kitao, F Hirata, N Go *J. Phys. Chem.* **97** 10231 (1993)
207. M Ullner, C E Woodward, B Jonsson *J. Chem. Phys.* **105** 2056 (1996)
208. B M Pettitt, M Karplus *Chem. Phys. Lett.* **121** 194 (1985)
209. J S Perkyns, Y Wang, B M Pettit *J. Am. Chem. Soc.* **118** 1164 (1996)
210. M Kinoshita, Y Okamoto, F Hirata *J. Am. Chem. Soc.* **120** 1855 (1998)

211. M Kinoshita, Y Okamato, F Hirata *J. Chem. Phys.* **110** 4090 (1999)
212. S Ten-no, F Hirata, S Kato *Chem. Phys. Lett.* **214** 391 (1993)
213. S A Maw, R A Bryce, R J Hall, A J Masters, I H Hillier *J. Phys. Chem. B* **102** 4089 (1998)
214. T Ishida, F Hirata, S Kato *J. Chem. Phys.* **105** 1546 (1996)
215. F Hirata *Bull. Chem. Soc. Jpn.* **71** 1483 (1998)
216. H Sato, F Hirata, A B J Myers *J. Phys. Chem. A* **102** 2065 (1998)
217. N Yoshida, S Kato *J. Chem. Phys.* **113** 4974 (2000)
218. H Sato, A Kovalenko, F Hirata *J. Chem. Phys.* **112** 9463 (2000)
219. T Ishida, F Hirata, S Kato *J. Chem. Phys.* **110** 3938 (1999)
220. Y Harano, H Sato, F Hirata *J. Am. Chem. Soc.* **122** 2289 (2000)
221. A K Pikaev *Sovremennaya Radiatsionnaya Khimiya. Radioliz Gazov i Zhidkostei* (Modern Radiation Chemistry. Radiolysis of Gases and Liquids) (Moscow: Nauka, 1986)
222. L Kevan, D F Feng *Chem. Rev.* **80** 1 (1980)
223. M Sprik, R W Impey, M L Klein *J. Stat. Phys.* **43** 967 (1986)
224. M Sprik, M L Klein *J. Chem. Phys.* **87** 5987 (1987)
225. A Wallqvist, D Thirumalai, J Berne *J. Chem. Phys.* **86** 6404 (1987)
226. A Wallqvist, G Martyna, J Berne *J. Phys. Chem.* **92** 1721 (1988)
227. J Schnitker, P J Rossky *J. Chem. Phys.* **86** 3462 (1987)
228. P J Rossky, J Schnitker *J. Phys. Chem.* **92** 4277 (1988)
229. P J Rossky, G S Del Biono, T H Murphrey *J. Phys. Chem.* **96** 6965 (1992)
230. G S Del Biono, P J Rossky, T H Murphrey *J. Phys. Chem.* **96** 7761 (1992)
231. A Mosyak, P J Rossky, L Turi *Chem. Phys. Lett.* **282** 239 (1998)
232. B J Schwartz, P J Rossky *J. Chem. Phys.* **105** 6997 (1996)
233. P Graf, A Nitzan, G H F Diercksen *J. Phys. Chem.* **100** 18 916 (1996)
234. D Chandler, P G Wolynes *J. Chem. Phys.* **74** 4078 (1981)
235. G Martyna, Z Deng, M L Klein *J. Chem. Phys.* **98** 555 (1993)
236. J Zhu, R Cukier *J. Chem. Phys.* **99** 5384 (1993)
237. G N Chuev *Usp. Fiz. Nauk* **169** 155 (1999) [*Physics-Uspekhi* **42** 149 (1999)]
238. G N Chuev, N Russo *Chem. Phys. Lett.* **368** 53 (2002)
239. G N Chuev, V V Sychyov, O Yu Sokolova *Phys. Rev. E* **63** 061204 (2001)
240. D Chandler, K Leung *Ann. Rev. Phys. Chem.* **45** 1500 (1994)
241. D Laria, D Wu, D Chandler *J. Chem. Phys.* **95** 4444 (1991)
242. S Miura, F Hirata *J. Phys. Chem.* **98** 9649 (1994)
243. J Jortner, R M Noyes *J. Phys. Chem.* **70** 770 (1966)
244. D F Feng, K Feuki, L Kevan *J. Chem. Phys.* **58** 3281 (1973)
245. H P Kaukonen, R N Barnett, U Landman *J. Chem. Phys.* **97** 1365 (1992)
246. N Nicoloso, W Freyland *J. Phys. Chem.* **87** 1997 (1987)
247. Z Deng, G Martyna, M L Klein *Phys. Rev. Lett.* **71** 267 (1993)
248. G N Chuev *Zh. Eksp. Teor. Fiz.* **118** 1134 (2000) [b]
249. V M Byakov, V I Grafutin, V L Grishkin, O V Il'yukhina, G G Myasishcheva, O P Stepanova, S V Stepanov, Yu V Funtikov *Khim. Fiz.* **18** 75 (1999) [c]
250. V M Byakov, S V Stepanov *Radiat. Phys. Chem.* **58** 687 (2000)
251. H Scmitz, T Müller-Plathe *J. Chem. Phys.* **112** 1040 (2000)
252. L Larrimore, R N McFarland, P A Sterne, A L R Bug *J. Chem. Phys.* **113** 10642 (2000)
253. G N Chuev, D M Schrader, S V Stepanov, V M Byakov *Int. J. Quantum Chem.* **88** 634 (2002)
254. F S Lee, Z-T Chu, M B Bolger, A Warshel *Protein Eng.* **5** 215 (1992)
255. J Åqvist, C Medina, J-E Samuelsson *Protein Eng.* **7** 385 (1994)
256. S R Edinger, C Cortis, P S Shenkin, R A Friesner *J. Phys. Chem. B* **101** 1190 (1997)
257. S Mente, M Maroncelli *J. Phys. Chem. A* **102** 3860 (1998)
258. Q Cui, M Karplus *J. Chem. Phys.* **112** (2000)
259. B J Schwartz, P J Rossky *J. Chem. Phys.* **101** 6902 (1994)
260. L Turi, A Mosyak, P J Rossky *J. Chem. Phys.* **107** 1970 (1997)
261. G N Chuev *Zh. Eksp. Teor. Fiz.* **105** 626 (1994) [b]
262. I V Kreitus *J. Phys. Chem.* **89** 1987 (1985)
263. M J Kamlet, J L M Abboud, W R Taft *Prog. Phys. Org. Chem.* **13** 485 (1981)
264. R Richert, A Wagener *J. Phys. Chem.* **97** 3146 (1993)
265. R F Loring *J. Phys. Chem.* **94** 513 (1990)
266. D V Matyushov, R Schmid, B M Ladanyi *J. Phys. Chem. B* **101** 1035 (1997)
267. S R Mente, M Maroncelli *J. Phys. Chem. B* **103** 7704 (1999)
268. A M Kjaer, J Ulstrup *J. Am. Chem. Soc.* **109** 1934 (1987)
269. K Coutinho, S Canuto, M C Zerner *Int. J. Quantum Chem.* **65** 885 (1997)
270. K Coutinho, S Canuto *Adv. Quantum Chem.* **28** 89 (1997)
271. K Coutinho, S Canuto, M C Zerner *J. Chem. Phys.* **112** 9874 (2000)
272. G van der Zwan, J T Hynes *J. Phys. Chem.* **89** 4181 (1985)
273. M J Maroncelli *Mol. Liq.* **57** 1 (1993)
274. M Horng, J Gardecki, A Papazyan, M Maroncelli *J. Phys. Chem.* **99** 17311 (1995)
275. C-P Hsu, X Song, R Marcus *J. Phys. Chem. B* **101** 2546 (1997)
276. B Bagchi, E W Castner, G R Fleming *J. Mol. Struct.* **194** 171 (1989)
277. M Basilevsky, D Parsons, M Vener *J. Chem. Phys.* **108** 1103 (1998)
278. X Song, D Chandler *J. Chem. Phys.* **108** 2594 (1998)
279. P G Wolynes *J. Chem. Phys.* **86** 5133 (1987)
280. I Rips, J Clafter, J Jortner *J. Chem. Phys.* **88** 3246 (1988)
281. I Rips, J Clafter, J Jortner *J. Chem. Phys.* **89** 4288 (1988)
282. B Bagchi, A Chandra *Adv. Chem. Phys.* **80** 1 (1991)
283. I Rips, in *Ultrafast Reaction Dynamics and Solvent Effects* (Eds Y Gaudel, P J Rossky) (New York: AIP Press, 1994) p. 334
284. A Kornyshev, A Kuznetsov, D Phelps, M Weaver *J. Chem. Phys.* **91** 7159 (1989)
285. X Song, R Marcus *J. Chem. Phys.* **99** 7768 (1993)
286. D F Parsons, M V Vener, M V Basilevsky *J. Phys. Chem. A* **103** 1171 (1999)
287. R A Marcus, N Sutin *Biochim. Biophys. Acta* **811** 265 (1985)
288. A M Kuznetsov, J Ulstrup *Electron Transfer in Chemistry and Biology* (Chichester: Wiley, 1999)
289. A M Kuznetsov *Charge Transfer in Physics, Chemistry and Biology* (Reading: Gordon and Breach, 1995)
290. M D Newton *Adv. Chem. Phys.* **106** 303 (1999)
291. G L Closs, L T Calcaterra, N J Green, K W Penfield, J R Miller *J. Phys. Chem.* **90** 3673 (1986)
292. J R Miller, B P Paulson, R Bal, G L Closs *J. Phys. Chem.* **99** 6923 (1995)
293. P Vath, M B Zimmt, D V Matyushov, G A Voth *J. Phys. Chem. B* **103** 9130 (1999)
294. D V Matyushov *Chem. Phys.* **211** 47 (1996)
295. D V Matyushov, G A Voth *J. Chem. Phys.* **111** 3630 (1999)
296. I Read, A Napper, M B Zimmt, D H Waldek *J. Phys. Chem. A* **104** 93 859 (2000)
297. A Napper, I Read, R Kaplan, M B Zimmt, D H Waldek *J. Phys. Chem. A* **106** 5288 (2002)
298. M Newton, M Basilevsky, I Rostov *Chem. Phys.* **232** 201 (1998)
299. M Basilevsky, I Rostov, M Newton *J. Electroanal. Chem.* **50** 69 (1998)
300. G L Closs, J R Miller *Science* **240** 440 (1988)
301. M V Basilevsky, G E Chudinov, I V Rostov, Y-P Liu, M Newton *J. Mol. Struct.* **371** 191 (1996)
302. K Kumar, I V Kurnikov, D N Beratan, D H Waldek, M B Zimmt *J. Phys. Chem. A* **102** 5529 (1998)
303. R A Kuharski, J S Bader, D Chandler, M Sprik, M L Klein, R W Impey *J. Chem. Phys.* **89** 3248 (1988)
304. J S Bader, R A Kuharski, D Chandler *J. Chem. Phys.* **93** 230 (1990)
305. A Warshel *J. Phys. Chem.* **86** 2218 (1982)
306. A K Churg, J-K Hwang, A Warshel *J. Am. Chem. Soc.* **109** 715 (1987)
307. R A Marcus *J. Chem. Phys.* **24** 966 (1956)
308. G King, A Warshel *J. Chem. Phys.* **93** 8682 (1990)
309. E A Carter, J T Hynes *J. Phys. Chem.* **93** 2184 (1989)
310. M Tachiya *J. Phys. Chem.* **93** 7050 (1989)
311. R B Yelle, T Ichiye *J. Phys. Chem. B* **101** 4127 (1997)
312. C Hartnig, M T M Kopera *J. Chem. Phys.* **115** 8540 (2001)
313. K Ando *J. Chem. Phys.* **106** 116 (1997)
314. K Ando *J. Chem. Phys.* **114** 9040 (2001)
315. K Ando *J. Chem. Phys.* **114** 9471 (2001)
316. J S Bader, C M Cortis, B J Berne *J. Chem. Phys.* **106** 2372 (1997)

317. L W Ungar, M D Newton, G A Voth *J. Phys. Chem. B* **103** 7367 (1999)
318. M Marchi, J N Gehlen, D Chandler, M D Newton *J. Am. Chem. Soc.* **115** 4178 (1993)
319. A Broo, S Larsson *Chem. Phys.* **148** 103 (1990)
320. R J Cave, M D Newton *J. Chem. Phys.* **106** 9213 (1997)
321. A A Stuchebrukhov *J. Chem. Phys.* **104** 8424 (1996)
322. A A Stuchebrukhov *J. Chem. Phys.* **107** 6495 (1997)
323. A A Stuchebrukhov *J. Chem. Phys.* **108** 8499 (1998)
324. I Daizadeh, J-X Guo, A A Stuchebrukhov *J. Chem. Phys.* **110** 8865 (1999)
325. W M Gelbart, A Ben-Shaul *J. Phys. Chem.* **100** 1369 (1996)

[a] — *Physics-Uspekhi (Engl. Transl.)*
[b] — *J. Exp. Theor. Phys. (Engl. Transl.)*
[c] — *Chem. Phys. Rep. (Engl. Transl.)*